European Journal of Pharmaceutical Sciences 171 (2022) 106123

Contents lists available at ScienceDirect

European Journal of Pharmaceutical Sciences

journal homepage: www.elsevier.com/locate/ejps

A new nanosuspension prepared with wet milling method for oral delivery of highly variable drug Cyclosporine A: development, optimization and in vivo evaluation

Sıla Gülbağ Pınar [a,b], Hande Canpınar [c], Çağman Tan [d], Nevin Çelebi [a,e,*]

[a] Gazi University, Faculty of Pharmacy, Department of Pharmaceutical Technology, Etiler, 06330, Yenimahalle, Ankara, Turkey
[b] Süleyman Demirel University, Faculty of Pharmacy, Department of Pharmaceutical Technology, 32260, Çünür, Isparta, Turkey
[c] Hacettepe University, Cancer Institute, Department of Basic Oncology, 06100, Sıhhiye, Ankara, Turkey
[d] Hacettepe University, Faculty of Medicine, Institute of Child Health, 06100, Sıhhiye, Ankara, Turkey
[e] Başkent University, Faculty of Pharmacy, Department of Pharmaceutical Technology, 06790, Etimesgut, Ankara, Turkey

ARTICLE INFO

Keywords:
Cyclosporine a
Nanosuspension
Top-down technology
Dissolution
Pharmacokinetic
T lymphocyte subsets

ABSTRACT

Cyclosporine A (CsA) is a cyclic polypeptide, that has been widely used for immunosuppression. This study aims to develop nanosuspension for oral administration of CsA using the wet milling (WM) method one of the top-down technologies. The WM method was optimized by studying the effects of critical process parameters for WM on the particle size (PS), particle size distribution (PDI), and zeta potential (ZP) of nanosuspensions using the Design of Experiment (DoE) approach. Nanosuspension was developed using hydroxypropyl methylcellulose (HPMC) and sodium dodecyl sulfate (SDS) and in vitro characterization studies were performed. In vitro dissolution and in vivo pharmacokinetic studies were conducted with biorelevant media (fasted and fed state simulated fluids) and fasted and fed states in rats, respectively. In vivo immunological studies were also performed. PS, PDI, and ZP values for nanosuspension were approximately 600 nm, 0.4, -25 mV, respectively. The solubility of CsA was increased by 4.5-folds by nanosuspensions. Dissolution studies showed that nanosuspension had higher dissolution than the commercial product in the FeSSIF medium. The pharmacokinetic study indicated that AUC_{0-24} values of CsA nanosuspension were to be 2.09 and 5.51-fold higher than coarse powder in fasted and fed conditions, respectively. Immunological studies were carried out after oral administration of nanosuspension for 21 days, the ratio of CD4+/CD8+ was found to be more acceptable than the commercial product. These results demonstrated that nanosuspension is a promising approach for increasing the bioavailability and avoiding the food effect on absorption of CsA which one of the highly variable drugs.

1. Introduction

Cyclosporine A (CsA) is a calcineurin inhibitor known for its immunomodulatory properties that prevent allograft rejection after organ transplantation and treat various inflammatory and autoimmune diseases (Guada et al., 2016). CsA is a neutral cyclic polypeptide that consists of 11 amino acids and has 1202 Daltons (Fig. 1 and Table 1). CsA binds to cyclophilin, forms cyclosporine-cyclophilin complex, and exhibits immunosuppressive activity by inhibiting T-cell activation and calcineurin phosphatase (Survase et al., 2011). CsA is classified as a Biopharmaceutical Classification System (BCS) Class II drug with low water solubility and high permeability (Amidon et al., 1995). Hence, there are many studies which aimed to increase the solubility, dissolution, and bioavailability of CsA (Gülbağ Pınar and Çelebi, 2019; Hermans et al., 2012; Italia et al., 2007). CsA has high variability in bioavailability, and its impact depends on the characteristics of the population. Factors such as age, gender, nutrients, and other drugs affect the distribution of CsA in the body and cause high intra-inter variability in pharmacokinetic parameters of CsA (Fahr, 1993; Flippin et al., 2000; Freeman, 1991). CsA is administered to patients with three routes; oral, ophthalmic, and intravenous. After oral administration, CsA is absorbed from the gastrointestinal tract, and its bioavailability varies between 20 and 60% (Christians and Sewing, 1993). CsA shows the maximum drug concentration is between 1 and 8 h after oral administration and is in the range of 2.9–4.7 L/kg for distribution in the human body (Lindholm, 1991). CsA active ingredient is widely used commercially under the

* Corresponding author at: Faculty of Pharmacy, department of Pharmaceutical Technology, Baskent University, Balca-Etimesgut, Ankara, Turkey.
E-mail address: fncelebi@baskent.edu.tr (N. Çelebi).

https://doi.org/10.1016/j.ejps.2022.106123
Received 6 July 2021; Received in revised form 30 December 2021; Accepted 3 January 2022
Available online 10 January 2022

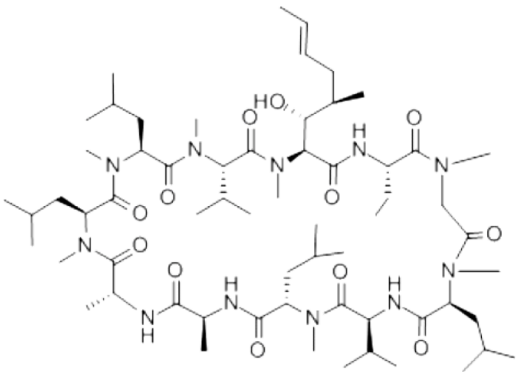

Fig. 1. Chemical structure of CsA.

Table 1
Physicochemical properties of Cyclosporine A.

Properties	Cyclosporine A
Chemical formula	$C_{62}H_{111}N_{11}O_{12}$ (*)
Molecular weight	1202 Dalton (*)
Log P	2.92 (*)
pKa (Strongest Acidic)	11.83 (**)
pKa (Strongest Basic)	−2.4 (**)
Physiological Charge	0 (**)
Isoelectrical point (pI)	9.6 (***)
Biopharmaceutical Classification System	Class II (****)

* Guada et al., 2016.
** PubChem Compound Summary – Cyclosporine A. 2021.
*** Handschumacher et al., 1984.
**** Amidon et al., 1995.

name of "Sandimmun Neoral®" by Novartis company, in a soft gelatin capsule and oral solution form. In addition to CsA, the commercial product components disclosed by Novartis are alpha-tocopherol, ethanol anhydrous, propylene glycol, corn oil-mono-di-triglycerides, and macrogol glycerol hydroxy stearate (Ph. . Eur)/ polyoxyl 40 hydrogenated castor oil (NF). There are ethanol and polyoxyl 40 hydrogenated castor oil in the commercial product composition to increase the solubility of CsA. Many formulation studies have been carried out and studies are continuing to avoid the use of ethanol and polyoxyl 40 hydrogenated castor oil in the commercial CsA formulation and to use cheaper and safer excipients.

Oral administration is preferable to other routes for safety, simplicity, comfort, and patient compatibility. However, fasted or fed situations may cause variability in the bioavailability of the drug which was administered orally (Cheng et al., 2019). Food affects the absorption of drugs by delaying gastric emptying time, changing gastrointestinal pH, stimulating the bile flow, increasing blood flow of organs, or physically interacting with drugs (Omachi et al., 2019). CsA is a drug that has fasted/fed and intra/inter-individual variability and there are many studies related to decreasing fasted/fed variability (Balandraud-Pieri et al., 1997; Yang et al., 2006).

Nanosuspensions (also called nanocrystals) are carrier-free colloidal drug delivery systems in the nanosized range and composed of 100% drug (Junghanns and Müller, 2008). Nanosuspensions were used for poorly soluble drugs such as BCS Class II and IV drugs for increasing solubility and bioavailability (Junyaprasert and Morakul, 2015). The production of nanosuspensions is basically divided into two technologies; top-down and bottom-up. The top-down technology consists of wet media milling (WM) and high pressure homogenization (HPH) methods. Large drug particles are reduced to nanoscale in these technologies. In another method, bottom-up technology, precipitation method is used and solid nanocrystals are obtained by precipitation of dissolved molecules for increasing bioavailability and efficacy of many drugs (Ao et al., 2020; Li et al., 2020, 2018). Also, combination methods in which several techniques are used together are interesting approaches in recent years (Ahire et al., 2018; Fu et al., 2013). Due to the numerous advantages of top-down production methods, such as using a minimum of the organic solvent and solvent residues, higher drug loading, increased stability, they are considered as the first alternative of preparation methods of nanosuspension (Möschwitzer, 2013). Many studies are using either wet media milling (Li et al., 2020; Gulsun et al., 2018; Huang et al., 2018; Koradia et al., 2018; Medarevic et al., 2018; Ding et al., 2019; Ghosh et al., 2012; Liu et al., 2020) or high pressure homogenization methods (Gülbağ Pınar and Çelebi, 2019; He et al., 2017; Karaküçük et al., 2016; Mauludin et al., 2009; Oktay et al., 2018; Karakucuk et al., 2020; Oktay et al., 2020) in the preparation of nanosuspensions of water insoluble BCS class II and IV drugs. Moreover, combining top-down and bottom-up techniques, as a more recent strategy, results in successful nanosuspensions (Attari et al., 2016; Hong et al., 2014; Patel et al., 2020; Zong et al., 2017). High pressure homogenization and wet milling are considered as suitable methods for preparing nanosuspensions of poorly soluble drugs and there are many pharmaceutical products produced by these methods in the market (Junghanns and Müller, 2008; Möschwitzer, 2013).

In light of this information, it was aimed to develop a CsA formulation by using cheaper, easily available, safe, and compatible excipients for the patient instead of ethanol and polyoxyl 40 hydrogenated castor oil found in the commercial product. For this purpose, the currently used nanosuspension formulations were preferred. The present study aimed to develop and evaluate CsA nanosuspension with stabilizer combination (polymeric and surfactant stabilizers) using the WM method with the Design of Experiment (DoE) approach for administrating orally. In this study, to reduce the cost of the microemulsion formulation of the commercial product (Sandimmun Neoral) in the soft gelatin capsule; the lyophilization process was carried out in the nanosuspensions prepared to present the solid form to the patient with a hard gelatin capsule. The characterization was investigated by particle size (PS), particle size distribution (PDI), zeta potential (ZP) measurement, differential scanning calorimetry (DSC), and X-ray powder diffraction (XRD) analysis. Morphological imaging was also performed with scanning electron microscopy (SEM). Solubility study was evaluated in distilled water with CsA nanosuspension and coarse CsA powder. In vitro dissolution studies were also evaluated in dissolution media and biorelevant media (fasted and fed state simulated fluids). Also, in vivo pharmacokinetic studies were performed with CsA coarse powder, physical mixture, the commercial product (Sandimmun Neoral®), and CsA nanosuspension in Wistar albino rats after being dispersed in water with fasted and fed state. Immunological evaluations were also performed in rats by comparing the effect of nanosuspension on T cell subgroups (CD3, CD4, CD8, CD19B, and CD56) and immune system cells (IL-2, IFN-gamma, TNF-alpha) with the commercial product at the end of the 21 day administration.

2. Materials and methods

2.1. Materials

Cyclosporine A, the model drug of this study, was a gift sample from Deva Drug Company (Turkey). The stabilizers used in this research were hydroxypropyl methylcellulose (HPMC) (3 cps) donated from Colorcon Limited (Turkey) and sodium dodecyl sulfate (SDS) purchased from Merck (Germany). D(-) Mannitol was obtained from Merck (Germany). SIF® Powder was purchased from Biorelevant (UK). CD3 FITC, CD4 FITC, CD8a FITC, CD19 FITC, and CD56 FITC anti-rat antibodies were purchased from Biolegend (USA). Multiplex bead kits were purchased from Invitrogen Inc. Camarillo, CA, USA (Invitrogen Ratplex invitrogen® Panel). All other ingredients and chemicals were analytical grade.

2.2. Preparation of CsA nanosuspension

CsA nanosuspension was prepared by WM process, which one of the top-down nanosuspension production technology, using a laboratory planetary ball mill (Retch PM100). The schematic presentation of preparation steps for nanosuspension is shown in Fig. 2. Firstly, HPMC (1% w/w) and SDS (0.5% w/w) were dissolved in deionized water. Then, 1% (w/w) of CsA was dispersed in this stabilizer solution under the magnetic stirrer at 1000 rpm for 20 min. The UltraTurrax (Heidolph, Silent Crusher M) (at 15,000 rpm- 10 min) was used to reduce the particle size of this coarse suspension. Finally, the suspension was transferred into a milling bowl containing different mill beads and milling was performed at room temperature for 1 hour.

The volume of the milling bowl is approximately 50 mL. 15 mL of the suspension prepared for the milling process was taken and transferred to the milling bowl. For milling, beads were added to the low, medium, or high milling bowl as indicated in Table 2. The remaining volume in the milling bowl (approximately 10 mL-20 mL remaining depending on the level) is required for rotational and impact forces during the milling process.

The different grinding bead volumes (X_1), (15 mL, 20 mL, and 25 mL), the different diameter of zirconium oxide beads (X_2) (0.1 mm, 0.5 mm, and 1 mm), and the different milling speeds (X_3) (200 rpm, 400 rpm, and 600 rpm) were identified as critical process parameters in preformulation studies and their effects on particle size (Y_1), particle size distribution (Y_2), and zeta potential (Y_3) were evaluated using DoE. Each factor was varied at three levels and 3^3 full factorial design, with two replicates, was applied to optimize the formulations (Table 2). After performing experiments in random order, results were analyzed using Design Expert.

2.3. Particle size, particle size distribution, and zeta potential determination

PS, PDI, and ZP analysis of nanosuspensions were performed at the end of milling using Malvern ZetaSizer (Malvern Instruments, UK) particle size analyzer at room temperature. The measurement was carried out by diluting the samples with distilled water. 750 μL of nanosuspensions were dropped into the sample cup and 750 μL of distilled water were added to measure. Each sample was measured at least three times.

2.4. Short-term physical stability

To investigate the effects of stabilizers on the physical stability of CsA nanosuspension, the short-term physical stability studies were carried at room temperature (25 °C). PS, PDI, and ZP values were measured after the preparation of nanosuspensions (at initial). The measurements were repeated after one week and one month of storage terms.

Table 2
Experiment design of the WM method.

Independent variables	Bead volume	Low: 15 mL Medium: 20 mL High: 25 mL
	Bead diameter	Low: 0.1 mm Medium: 0.5 mm High: 1 mm
	Milling speed	Low: 200 rpm Medium: 400 rpm High: 600 rpm
↓		
Dependent variables	Particle size (PS) Particle size distribution (PDI) Zeta potential (ZP)	

2.5. Lyophilization of nanosuspension

The solidification of nanosuspensions is important for long-term stability and solid dosage forms such as tablet, capsule, pellet, and effervescent tablet. The lyophilization (freeze drying) process which one of the solidification methods was applied after the PS, PDI, and ZP measurements of CsA nanosuspension. D(-) Mannitol was used as a cryoprotectant in the prepared nanosuspension and the ratio of CsA: mannitol was selected as 1:1 (% w/w). For the lyophilization process, about 2 g of the nanosuspension were frozen at −80 °C for 2 h, and freeze drying was carried out at −50 °C under 0.021 mbar pressure for 48 h (Christ Alpha 1–2 LD Plus).

2.6. Preparation of the physical mixture

The physical mixture was prepared by mixing the CsA coarse powder for about 5 min at the same rate as the stabilizers (HPMC:SDS 1:0.5%) were used in the nanosuspension formulations. Mannitol, which is also used as a cryoprotectant, is present in the physical mixture at a rate of 1%. The physical mixture was used to prove the effect of nanosuspension and to evaluate the dissolution profile of stabilizers in dissolution studies and the pharmacokinetic effect of stabilizers in rats.

2.7. Characterization studies

2.7.1. Differential scanning calorimetry

DSC analysis was carried out to investigate the effect of stabilizers, the physical mixture, and nanosuspension on the internal structure of the system during the preparation of the nanosuspension. Thermal properties of CsA, stabilizers, the physical mixture, and lyophilized CsA nanosuspension were examined by DSC (Shimadzu Scientific Instruments). Samples were weighed 2 mg and placed in an aluminum pan and then the pan was sealed with a press. DSC thermograms were obtained with a heating rate of 10 °C/min and temperatures between 25 °C

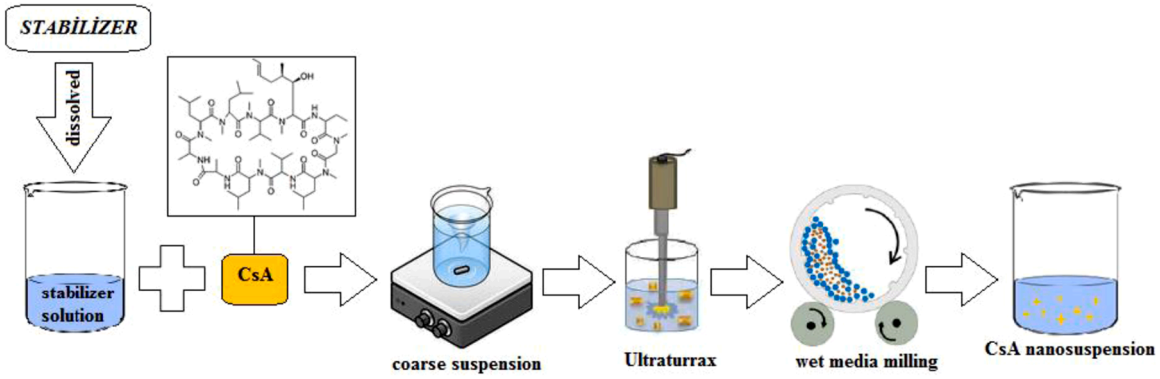

Fig. 2. The flowchart of the preparation steps for the WM method.

and 200 °C.

2.7.2. X-ray diffractometry

XRD analysis was performed on lyophilized CsA nanosuspension, CsA coarse powder, stabilizers, and physical mixture to detect possible changes in the internal structure of lyophilized CsA nanosuspension. In XRD analysis, the scan rate was set to 1° per minute and the scan range was 2θ in the range of 3–90° (Rigaku Ultima IV, Japan).

2.7.3. Scanning electron microscopy

Scanning electron microscopy (SEM) was used to evaluate the morphological images of the lyophilized nanosuspension and to compare the morphological characteristics of CsA coarse powder and physical mixture. All samples were mounted on a brass stage using adhesive carbon tape and coated with gold-palladium before measurement. The imaging studies were performed using a scanning electron microscope (Quanta 400F).

2.8. Solubility study

The solubility of CsA coarse powder, the physical mixture, and the lyophilized CsA nanosuspension (nanocrystal) were examined in distilled water. Solubility measurements were carried out as follows: firstly excessive amounts of CsA powder, the physical mixture, and lyophilized nanosuspension were added to distilled water in 10 mL capped vials and shaken for 48 h at 37±0.5 °C. Then the samples were filtrated through a 0.22 μm filter (Merck Millipore®, Germany) and the CsA concentration of filtrates was analyzed by UV spectrophotometric method at 207 nm. UV spectrophotometric method was validated according to accuracy, precision, repeatability, linearity, specificity, detection limit, quantitation limit, and range. Experiments were carried out in triplicate and solubility results were calculated as the mean±standard deviation (SD).

2.9. In vitro dissolution study

Considering the dissolution method of the commercial product (Sandimmun Neoral®) reported in USP, in vitro dissolution studies were carried out using USP Apparatus I Basket, rotating at 150 rpm and a temperature of 37±0.5 °C (Xu et al., 2013). The dissolution studies were conducted in 1000 mL of 0.1 N HCl containing 0.5% SDS and 0.1 N HCl without SDS. The dissolution studies were also performed in 500 mL of FaSSIF and FeSSIF media containing different amounts of sodium taurocholate and phospholipids to simulate the in vivo fasted and fed state, respectively. Accurate weight of CsA coarse powder, physical mixture, and CsA nanosuspension equivalent to 10 mg CsA and put into hard gelatin capsules (number:00EL). To show the effect of the nanosuspensions on dissolution, in vitro dissolution studies were performed with biorelevant media CsA coarse powder, physical mixture, CsA nanosuspension, and the commercial product (Sandimmun Neoral®). Biorelevant media (FaSSIF and FeSSIF) were prepared according to the protocols of Biorelevant.com. Samples were dropped into vessels containing 500 mL of FaSSIF and FeSSIF media to simulate the in vivo fasted and fed state and withdrawn at predetermined times of 5, 10, 20, 30, 45, 60, 90, and 120 min. An equal volume of fresh medium was added to maintain sink conditions. The dissolution of each sample was performed in triplicate. The samples were filtered using a 0.22 μm membrane filter (Merck Millipore®, Germany) and the concentration of CsA in samples was determined at 205 nm wavelength using the HPLC method. The dissolution profiles were evaluated by cumulative drug dissolved (%) to time and the mean values and standard deviations were reported.

2.10. Pharmacokinetic studies in rats

In vivo pharmacokinetic studies were performed on male Wistar albino rats (body weight 220 ± 20 g) in accordance with Gazi University Local Ethics Committee for Animal Experiments (66,332,047–604.01.02). The animals were kept in a controlled temperature of 25±3 °C, and relative humidity of 60±5%, in a 12-hour dark/light cycle. The rats were allowed to acclimatize for one week before the experiment. All animals were divided into fasted and fed groups since the bioavailability of CsA in the case of fasted/fed was variable. Rats are divided into five groups (control, CsA coarse powder, physical mixture, commercial product, and CsA nanosuspension) in fasted and fed states. When in the fasted group no food was given to animals 12 h before and 6 h after the administration of the dose, animals were fed ad libitum in the fed group. All groups of animals free access to water during experiments. Drug administration for all groups was carried out early in the morning so that rats fed at night were considered to have a similar level of satiety and to minimize intra-group variation. CsA coarse powder, physical mixture, CsA nanosuspension, and commercial product (Sandimmun Neoral®) were suspended in 1 mL of distilled water. Samples were administered orally at 10 mg/kg of CsA in rats with the help of oral gavage as a single dose (da Silva Peralta et al., 2015; Iyama et al., 2019; Lahiani-Skiba et al., 2018).

Blood samples (200 μL) were collected from the tail vein using a restrainer at each time point (0, 0.5, 1, 2, 4, 8, and 24 h) into heparinized microcentrifuge tubes. The plasma samples were centrifuged at 8000 rpm for 15 min immediately. Supernatants were separated and stored at −80 °C until analysis.

Precipitation was performed with the organic solvent to determine the plasma concentration of CsA. For extraction, 10 μL of internal standard (loratadine) at a concentration of 5 μg/mL was added into 50 μL of rat plasma. Vortexing was performed for 30 s and then 450 μL of acetonitrile was added. The mixture was vortexed for 5 min and centrifuged at 4 °C for 10 min at 15,300 rpm. Finally, the upper phase was taken and injected into the device.

The pharmacokinetic parameters including the area under the curve (AUC), the maximum plasma concentration (C_{max}), the time of the maximum plasma concentration (t_{max}), the half-life time ($t_{1/2}$), and the mean residence time (MRT) were calculated using WinNonlin® Professional (Phoenix WinNonlin 7.0, USA).

2.11. Analytical methods

Different analytical methods such as UV spectrophotometer, HPLC, and LC-MS/MS systems were used to analysis of CsA in different studies. The CsA concentration in solubility, dissolution, and pharmacokinetic studies were determined with UV spectrophotometer, HPLC, and LC-MS/MS analysis, respectively.

2.11.1. UV spectrophometer analysis of CsA

The CsA concentration was analyzed by UV spectrophotometric method at 207 nm wavelength in solubility experiments. Due to the low solubility of CsA in distilled water, the quantification was made in methanol:distilled water (1:1) media. The UV method was validated for parameters such as specificity, linearity, range, accuracy, precision, and robustness.

2.11.2. HPLC analysis of CsA

The CsA concentration of dissolution studies was estimated by HPLC (Agilent 1220 Infinity, USA) using C18 RP column (150 mm x 4.6 mm, 5 μm) at 205 nm using UV detector (Aljohani et al., 2017). The mobile phase consisted of methanol and water (75:25) and a flow rate of 1.0 mL/min (Xu et al., 2013; Basaran et al., 2014). The column temperature was maintained at 60 °C, and the injection volume was 20 μL. The HPLC method was validated according to validation parameters (accuracy, precision, repeatability, linearity, specificity, detection limit, quantitation limit, and range).

2.11.3. LC-MS/MS analysis of CsA

Plasma samples were analyzed by the LC-MS/MS method (Shimadzu

UFLC & AB Sciex API 4000) after a liquid phase extraction procedure. The chromatographic system consisted of a vacuum degasser, a binary pump, an autosampler, and a C18 column (100 mm x 2.1 mm, 3 μm, Thermo Scientific® Hypurity, USA) was used at 60 °C. As a mobile phase, 0.1% (w/w) formic acid solution containing 10 mM ammonium formate (A) and acetonitrile (B) were used. The flow rate was 1 mL/min with gradient method and the injection volume was 5 μL. In LC-MS/MS analysis, loratadine was used for the internal standard. The gradient conditions were set as follow: 0–1.20 min, 50% A; 1.20–1.21 min, 50–95% A; 1.21–3.50 min, 95% A; and 3.50–5.0 min, 50% A. Specific m/z 1219 and 383 $[M + H]^+$ was detected for CsA and loratadine, respectively.

2.12. Immunological evaluation

The in vivo immunological study was performed on 12 male Wistar albino rats (approximately 200–220 mg) which have been approved by Gazi University Local Ethics Committee for Animal Experiments (66,332,047–604.01.02). Rats were divided into four groups (3 rats in per group), and food and water were not restricted during the study. Formulations were applied by oral gavage at a dose of 10 mg/kg body weight CsA. The optimum CsA nanosuspension and the commercial product were dispersed in 0.5 mL deionized water before administration. Animals in groups one, two, and three were administered optimum CsA nanosuspension once a day for 7, 14, and 21 days, respectively. Rats in group four were administered the commercial product orally, once a day for 21 days. Blood samples (2 mL) were collected at 7, 14, and 21 days following administration.

2.12.1. Lymphocyte subsets and analysis of flow cytometry

Blood samples from rats were collected into ethylenediaminetetraacetic acid-anticoagulated (EDTA) tubes at 7, 14, and 21 days following the administration for analysis of flow cytometry. CD3 T cells, CD4 T helper cells, CD8 cytotoxic T cells, CD19 B cells, and CD56 Natural Killer (NK) cell surface expression analyses were performed by flow cytometry (Beckman Coulter Epics XL-MCL). Briefly, 100 μL of whole blood were incubated with 10 μL CD3 FITC (Biolegend clone 1F4), 10 μL CD4 FITC (Biolegend clone W3/25), 10 μL CD8 FITC (Biolegend clone 0 × 8), 10 μL CD19 FITC (BD Biosciences clone 1D3), 10 μL CD56 monoclonal antibodies (Abcam clone RNL), and isotopic controls (MsIgG1 FITC, Biolegend; MsIgM FITC, Biolegend and MsIgG2FITC, Biolegend) for 10 min at room temperature. After the incubation, peripheral blood mononuclear cells were lysed using Immunoprep solution (Beckman Coulter). The cells were analyzed on an EPICS XLMCL flow cytometer (Beckman Coulter) and then 10,000 events were acquired through a live gate drawn on forward light scatter and side light scatter. The percentage of CD3+, CD4+, CD8+, CD19+, and CD56+ cells was calculated according to the isotype stainings.

2.12.2. Immune cell subsets and analysis of multiplex immunoassay

The samples with different experimental groups were kept at room temperature before using. The determination of IL-2, IFN-γ, and TNF-α levels in the experimental group samples was made by RAT Cytokine-Plex Panel kit using the Luminex-200TM device in accordance with the manufacturer's recommendations (Invitrogen, USA). The total amounts of cytokines were determined as picogram/microliter (pg/μl). Analyzes were done "Invitrogen ProcartaPlex Analyst software for the LuminexxMAP, MAGPIX, Bio-Plex®, MSD&Applied BioCode Platform". The concentrations of cytokines in serum samples using the Luminex 200TM instrument were determined. The assay was performed according to the manufacturer's instructions with Luminex laser-based fluorescent analytical test instrumentation. The concentrations of the samples were determined from the standard curve using curve fitting ProcartaPlex Analyst software. Standard curves for each cytokine were generated by using the reference cytokine concentrations supplied by the manufacturer.

2.13. Statistical analysis

Statistical analysis was performed using SPSS software (version 22.0, IBM Corp., USA). Data were presented as mean±standard deviation (SD). The significant difference was considered to be significant at $p< 0.05$ for all analyses.

3. Results and discussion

There are basically two different methods for the preparation of nanosuspensions as top-down and bottom-up methods. Many studies are conducted in recent years with one of these methods, the wet milling technique, which is one of the top-down methods (Gulsun et al., 2018; Huang et al., 2018; Koradia et al., 2018; Medarevic et al., 2018; Ding et al., 2019; Ghosh et al., 2012; Liu et al., 2020). In this study, CsA nanosuspensions were prepared by wet milling technique and a combination of HPMC and SDS was used as a stabilizer. In the following section, the results of the optimization studies with DoE are given, the optimum formulation has been decided from the surface response graphs obtained at the end of the DoE and further studies have been carried out with this optimum formulation.

3.1. Particle size, particle size distribution, and zeta potential measurement

After the preformulation study 54 formulations (3^3 factorial designs and 2 replicates) with low, medium, and high levels of independent variables were prepared with random design. Contour plots of PS, PDI, and ZP results of these formulations are given in Fig. 3.

As shown in Table 3, the interaction of milling speed, bead diameter, and bead volume in terms of PS was investigated and bead diameter ($p:<0.0001$) and milling speed ($p:0.0035$) were found to be significant variables. Thus, the PS varies depending on the changes in bead diameter and milling speed. The interaction equation for the model affecting the particle size (PS), A: milling speed, B: bead diameter, C: bead volume, AB: interaction of A and B, AC: interaction of A and C, and BC: interaction of B and C, is shown in Eq. (1).

$$\mathbf{PS} = +\mathbf{1270.52} - \mathbf{215.55} * \mathbf{A} + \mathbf{471.00} * \mathbf{B} - \mathbf{33.04} * \mathbf{C} - \mathbf{142.17} * \mathbf{AB} + \mathbf{176.79} * \mathbf{AC} + \mathbf{44.13} * \mathbf{BC} \quad \text{(Eq. 1)}$$

The interaction of milling speed, bead diameter, and bead volume in terms of PDI was investigated and bead diameter ($p:<0.0001$) and milling speed ($p:0.0203$) were found to be significant variables (Table 3). Hence, bead diameter and milling speed were the major factors affecting the PDI. The interaction equation for the model affecting the particle size distribution (PDI), A: milling speed, B: bead diameter, C: bead volume, AB: interaction of A and B, AC: interaction of A and C, BC: interaction of B and C, A^2: interaction of A and A, B^2: interaction of B and B and C^2: interaction of C and C, is shown in Eq. (2).

$$PDI = +0.43 - 0.034 * A + 0.086 * B - 0.023 * C - 0.038 * AB + 0.019 * AC - 0.019 * BC + 0.12 * A^2 - 9.231E - 003 * B^2 - 0.035 * C^2 \quad \text{(Eq. 2)}$$

The interaction of milling speed, bead diameter, and bead volume in terms of ZP was investigated and milling speed (p:0.0023) was found to be a significant variable (Table 3). Therefore, the ZP varies depending on the changes in milling speed. The interaction equation for the model affecting the zeta potential (ZP), A: milling speed, B: bead diameter, C: bead volume, AB: interaction of A and B, AC: interaction of A and C, BC: interaction of B and C, A^2: interaction of A and A, B^2: interaction of B and B and C^2: interaction of C and C, is shown in Eq. (3).

Considering DoE data; it was concluded that the optimum CsA nanosuspension with the WM method would be obtained by 1 hour milling with high milling speed (600 rpm), low bead size (0.1 mm), and high bead volume (25 mL). As a result of the WM process performed with 600 rpm milling speed, 0.1 mm bead diameter, and 25 mL bead volume, which is accepted as the optimum process parameters as a result of the DoE study, particle size, particle size distribution, and zeta potential has been obtained 561.2 ± 31.3, 0.374 ± 0.037, and −24.4 ± 0.9

$$ZP = -22.50 - 1.20 * A + 0.47 * B - 0.11 * C - 0.28 * AB - 0.69 * AC - 0.17 * BC - 1.76 * A^2 + 0.44 * B^2 - 1.27 * C^2 \quad \text{(Eq. 3)}$$

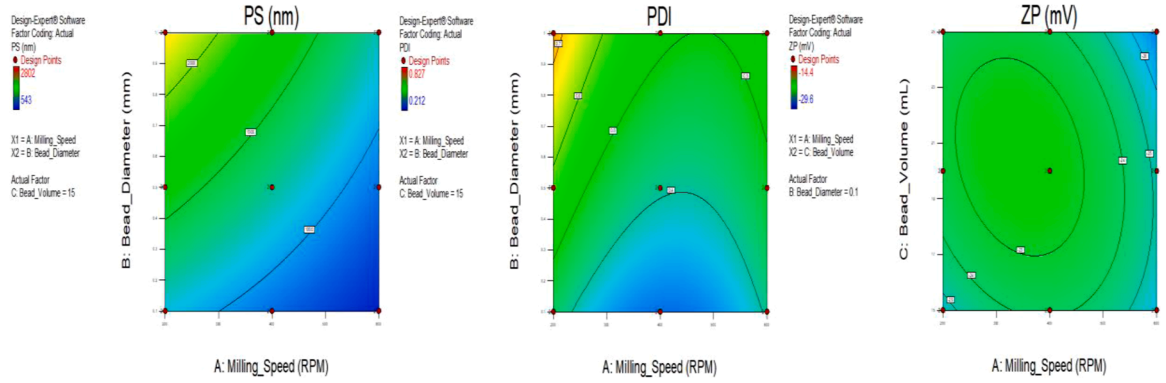

Fig. 3. Contour plots demonstrating the effects of the milling speed, bead diameter, and bead volume on PS, PDI, and ZP values.

The ANOVA results were evaluated in terms of PS, PDI, and ZP values of nanosuspension prepared with the WM method; while the variation of the bead volume did not cause significant change on the PS value, a significant decrease in PS value was observed by increasing milling speed (400 rpm and above), decreasing bead size (0.5 mm and 0.1 mm), and increasing bead volume (20 mL and above). While PDI values were decreased by increasing milling speed (300 rpm and above) and decreasing bead size (0.5 mm and 0.1 mm); there was no change observed in PDI values for all three bead volumes (15 mL, 20 mL, and 25 mL). When evaluated in terms of ZP values, although all ZP values obtained were above −20 mV and optimum for nanosuspension, the ZP value increased as the milling speed increased.

In a study by Zuo et al., esculetin nanosuspensions with low water solubility were produced by the wet milling method and the relationship between formulation parameters and process parameters was determined by the DoE approach. An esculetin-Povacoat ™ nanocrystal formulation with a 200 nm particle size was successfully obtained with specific critical process parameters and formulation composition within the design space after the DoE approach (Zuo et al., 2019).

In a study conducted to prepare etodolac nanosuspension (ETD-NS), the wet milling method was used and the process parameters were determined as 2 hour rotation time, 400 rpm rotation speed, 20 ml volume and 0.5 mm zirconium oxide bead diameter. The ETD-NS with approximately 190 nm particle size (PS), 0.16 polydispersity index (PDI), and 15 mV zeta potential (ZP) values were obtained (Karaküçük et al., 2021).

mV, respectively. Nanosuspensions for characterization studies and in vivo studies have been repeatedly prepared with these parameters. PS, PDI, and ZP values of each formulation were measured after preparation and they were found to be by the average accepted (PS, PDI, and ZP values for nanosuspension were approximately 600 nm, 0.4, −25 mV, respectively).

In further studies, CsA nanosuspensions prepared by this method using these variables were cited with the WM formulation code.

Table 3
ANOVA and interaction for PS, PDI, and ZP results of CsA: HPMC: SDS nanosuspension.

Source	PS		PDI		ZP	
	F value	P-value	F value	P-value	F value	P-value
Model	*10.31*	*<0.0001*	*8.56*	*<0.0001*	*2.98*	*0.0074*
A-Milling speed	*9.44*	*0.0035*	*5.80*	*0.0203*	*10.46*	*0.0023*
B-Bead diameter	*45.36*	*<0.0001*	*36.54*	*<0.0001*	*1.60*	*0.2128*
C-Bead volume	*0.22*	*0.6399*	*2.59*	*0.1148*	*0.082*	*0.7765*
AB	*2.76*	*0.1036*	*4.79*	*0.0340*	*0.37*	*0.5466*
AC	*4.24*	*0.0450*	*1.18*	*0.2842*	*2.31*	*0.1354*
BC	*0.27*	*0.6088*	*1.23*	*0.2737*	*0.13*	*0.7163*
A^2	–	–	*23.44*	*<0.0001*	*7.52*	*0.0088*
B^2	–	–	*0.14*	*0.7147*	*0.45*	*0.5043*
C^2	–	–	*2.05*	*0.1589*	*3.91*	*0.0542*

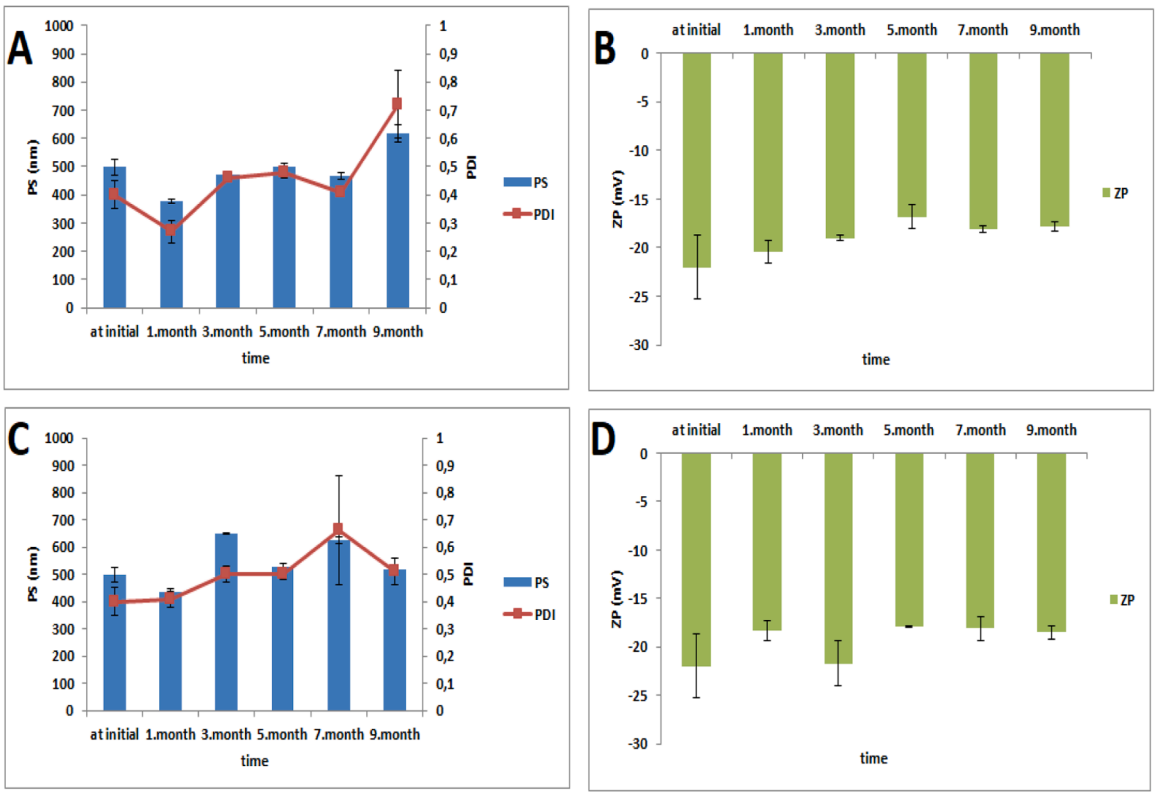

Fig. 4. PS, PDI, and ZP values of lyophilized CsA nanosuspension prepared by WM method (A: PS and PDI values at 4 °C, B: ZP values at 4 °C, C: PS and PDI values at 25 °C, D: ZP values at 25 °C).

3.2. *Short-term physical stability*

The short-term physical stability study of optimum CsA nanosuspension prepared with the WM method was performed by measuring PS, PDI, and ZP values at 25 °C for one month. There were no significant changes after one-month storage of optimum CsA nanosuspension prepared with the WM method on PS and PDI as they were approximately 700 nm and 0.4, respectively, similar to initial values. The ZP values were measured approximately at −26 mV for one week and one month. As a result of the physical stability study, the small particles did not cause a significant increase in the particle size (Ostwald ripening effect). Therefore, the zeta potential above −20 mV showed that the formulation was physically stable. HPMC and SDS were used as polymeric and surfactant stabilizers in nanosuspension to develop a stable formulation. Many studies are indicating that more stable nanosuspensions similar to our formulation are obtained when stabilizers are used in combination (Karaküçük et al., 2016; Zuo et al., 2013; Toziopoulou et al., 2017). After the measurement of PS, PDI, and ZP results of CsA nanosuspension, they were found approximately 600 nm, 0.4, and −25 mV, respectively.

To determine the stability after the lyophilization process, a stability

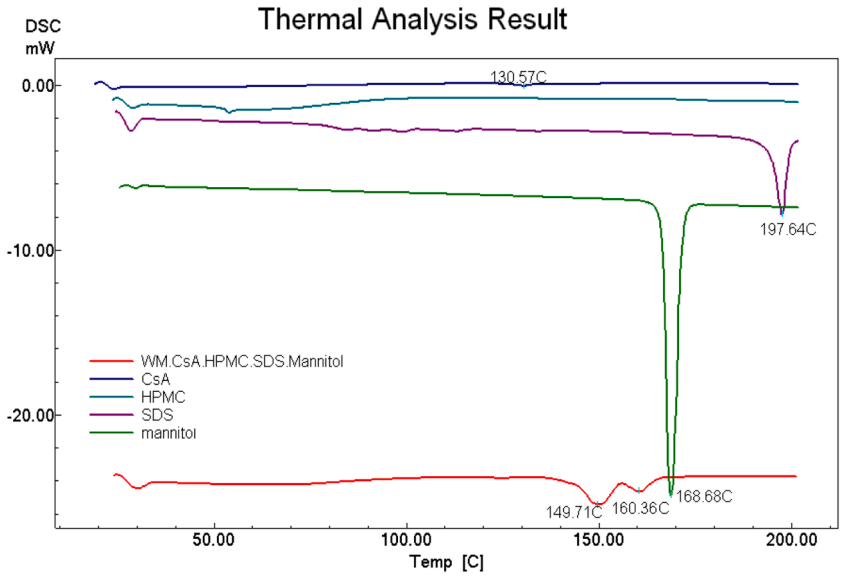

Fig. 5. DSC thermograms of CsA, HPMC, SDS, mannitol, and CsA nanosuspension prepared by WM method.

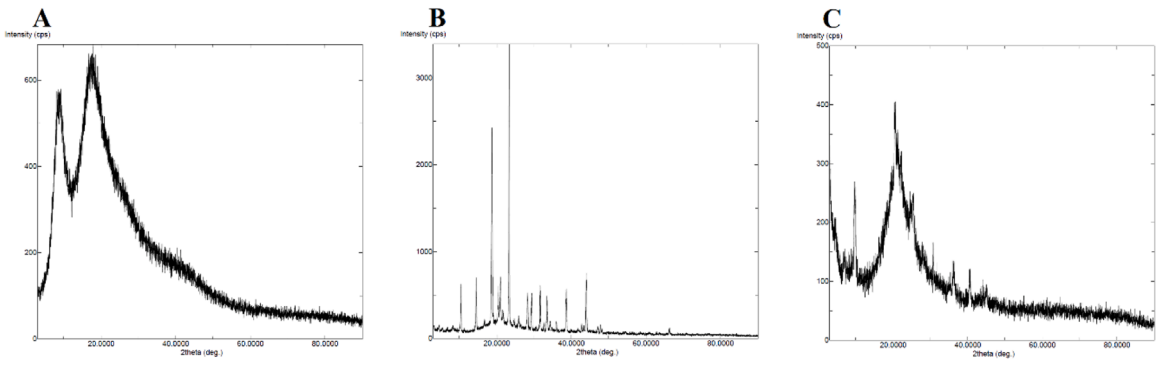

Fig. 6. X-ray diffraction patterns of CsA coarse powder (A), physical mixture (B), and CsA nanosuspension.

study was performed on lyophilized nanosuspension and the results are shown in Fig. 4. As a result of the stability studies carried out at 4 °C and 25 °C temperatures at the initial and at certain intervals during 9 months; similar results were found in PS, PDI, and ZP values in lyophilized WM nanocrystals at both temperatures, the nanosuspension proved to be stable.

3.3. Differential scanning calorimetry

Polymorphic changes of the active ingredient and stabilizers used were observed with DSC thermograms. DSC thermograms of CsA, excipients, and CsA nanosuspension prepared with WM method are shown in Fig. 5. From the DSC thermogram, CsA showed a small endothermic peak at 130.7 °C, which is in the range of literature values for the melting point of CsA (Jain et al., 2011; Onoue et al., 2010; Yamasaki et al., 2011). As the stabilizers (HPMC and SDS) and cryoprotectant (mannitol) used for nanosuspension covered the active ingredient all around, the peak of CsA could not be seen. There are many studies in the literature that the melting peak of the drug disappeared due to the effects of the excipients used in the formulation (Gulsun et al., 2018; Iyama et al., 2019; Jain et al., 2011).

3.4. X-ray diffractometry

The crystal properties of CsA, physical mixture, and CsA nanosuspension were investigated by X-ray diffractometry (XRD) (Fig. 6).

As it is shown in Fig. 6A, CsA was found to be amorphous, which was reported in the literatüre (Iyama et al., 2019; Yamasaki et al., 2011). While the crystal and amorphous structures of CsA, HPMC, and SDS, which are substances in the diffractogram of the physical mixture were appearing in Fig. 6B, the amorphous structure of the drug was determined in CsA nanosuspension Fig. 6C. It has been found that the crystalline ziprasidone active substance turns into an amorphous structure after the ball mill process and there is an increase in solubility (Zakowiecki et al., 2015).

Table 4
Saturation solubility of CsA coarse powder, physical mixture, and CsA nanosuspensions (mean±SD; $n = 3$).

Sample	Saturation solubility (μg/mL)
CsA coarse powder	*6.48 ± 0.88*
Physical mixture	*8.78 ± 0.38*
CsA nanosuspension	*29.41 ± 7.56*

3.5. Scanning electron microscopy

Scanning electron microscopy was used for the morphological examination of CsA coarse powder, physical mixture, and CsA nanosuspension (Fig. 7A-C). According to Fig. 7A, CsA coarse powders showed rod-like shapes. HPMC has been viewed as a long fiber and SDS globally. Mannitol, which is used for cryoprotectant purposes, has a crystal and spiny structure. The characteristic structures of the substances described above were observed in the SEM images of the physical mixture (Fig. 7B). CsA nanosuspensions prepared by the WM method were spherical and more homogeneous (Fig. 7C). This morphological change in the CsA coarse powder is thought to be caused by the grinding energy applied during the preparation with the WM method (Gülbağ Pınar and Çelebi, 2019; Tashan et al., 2019).

3.6. Solubility study

The saturation solubility study was carried out with CsA coarse powder, physical mixture, and lyophilized CsA nanosuspensions on a water bath at 37 °C. As shown in Table 4, the maximum solubility was found to be 6.48±0.88 μg/mL for CsA coarse powder and 8.78±0.38 μg/mL for the physical mixture. The solubility result for CsA nanosuspension prepared with WM was 29.41±7.56 μg/mL. These results showed that the WM method caused a 4.5-fold increase in solubility compared to the coarse powder. Thus, it is very clear that nanosuspension is an effective approach for improving the solubility of CsA.

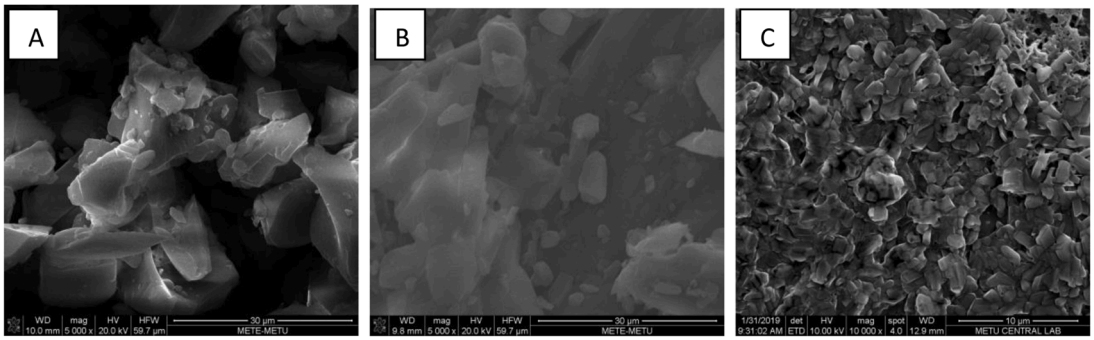

Fig. 7. SEM images of (A) CsA coarse powder (mag. 5000 x), (B) the physical mixture (mag. 5000x), and (C) CsA nanosuspension (mag. 10000x).

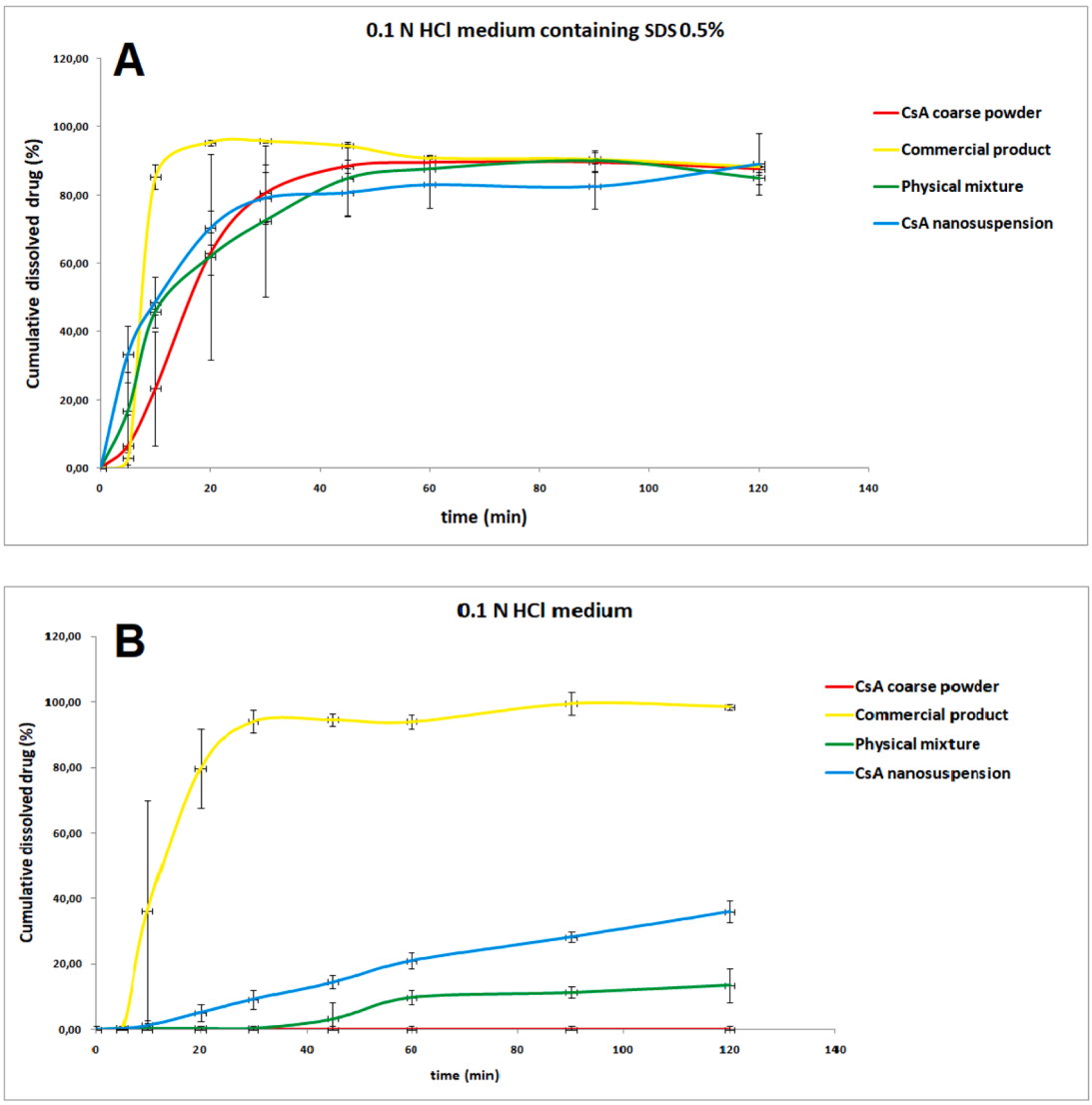

Fig. 8. Dissolution profiles of CsA coarse powder, physical mixture, CsA nanosuspension, and the commercial product in (A) 0.1 N HCl medium containing 0.5% SDS and (B) 0.1 N HCl medium.

This increase in solubility is considered to be due to the increase the saturation solubility and the increase of dissolution. The increase of the surface area of the particles brought to nanometer size according to the Ostwald-Freundlich equation is also considered as the reason for the solubility enhancement (Müller et al., 2011). Lastly, the stabilizers such as SDS used during the preparation of nanosuspensions may increase solubility.

The solubility of nanosuspensions increased up to 13.0-fold in comparison with micronized etodolac in nanosuspensions prepared using wet milling (Karaküçük and Çelebi, 2020). In a study, CsA nanosuspensions were developed by the pearl milling technique using poloxamer 407 as a stabilizer for intravenous administration and it was found that saturation solubility of CsA increased 5.69-fold (Nakarani et al., 2010). Differently in this research, optimum nanosuspensions for oral administration of CsA were obtained by using HPMC and SDS stabilizers in combination, and the effect of the process parameters with the DoE approach was examined in the WM method in our study and comprehensive in vitro and in vivo evaluation were performed.

3.7. *In vitro dissolution study*

In vitro dissolution studies were performed in four different media with CsA coarse powder, physical mixture, the commercial product, and CsA nanosuspension. 0.1 N HCl medium containing 0.5% SDS, recommended by FDA and USP for the commercial product, was used for dissolution studies (Xu et al., 2013). The filtration process is frequently used in vitro dissolution studies for filtration of aliquots (Kobayashi et al., 2020; Yamasaki et al., 2011; Onoue et al., 2010) and the filtration step did not affect the concentration of CsA in aliquots in our study. According to Fig. 8 and Fig. 10; 100% cumulative dissolved drugs were obtained with the commercial product and CsA nanosuspension, respectively (it seems that the filters used for filtration do not retain the active substance). The commercial product dissolved rapidly around 10 min in this medium; on the other hand, CsA coarse powder and physical mixture displayed about 80% dissolution in 120 min (Fig. 8A). Dissolution of nanosuspensions was lower compared to both the commercial product and physical mixture.

In vitro dissolution study was also performed with 0.1 N HCl to evaluate the effect of nanosuspensions on dissolution, considering that the high dissolution in 0.1 N HCl containing 0.5% SDS would be due to SDS in the medium. As shown in Fig. 8B, according to the dissolution results in 0.1 N HCl medium; while the CsA coarse powder did not show any dissolution, the physical mixture showed 10% dissolution at the end of the 120-minute-experiment period. The commercial product showed

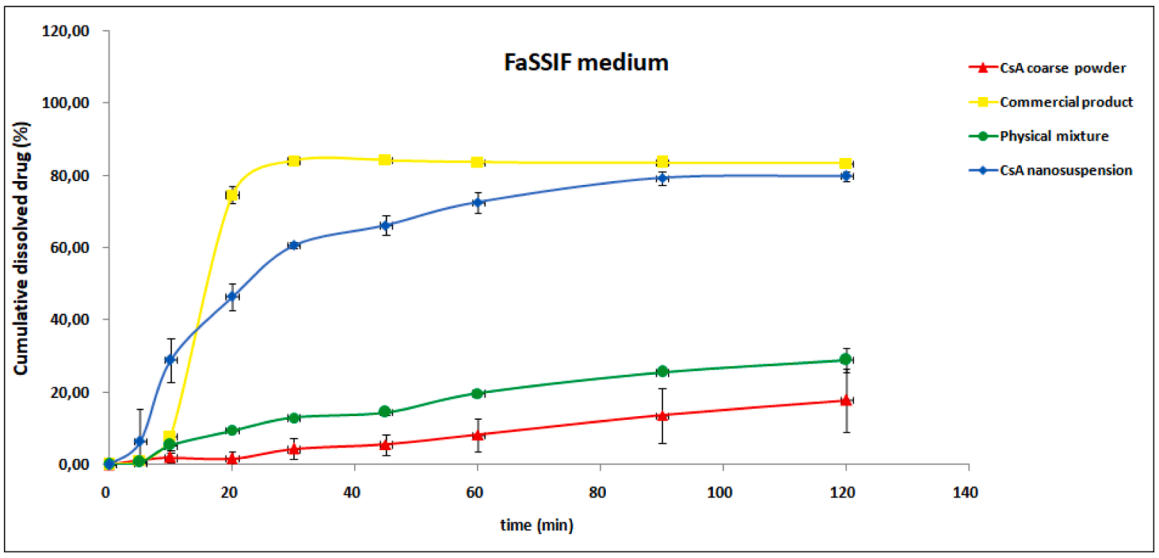

Fig. 9. Dissolution profiles of CsA coarse powder, physical mixture, CsA nanosuspension, and the commercial product in FaSSIF medium.

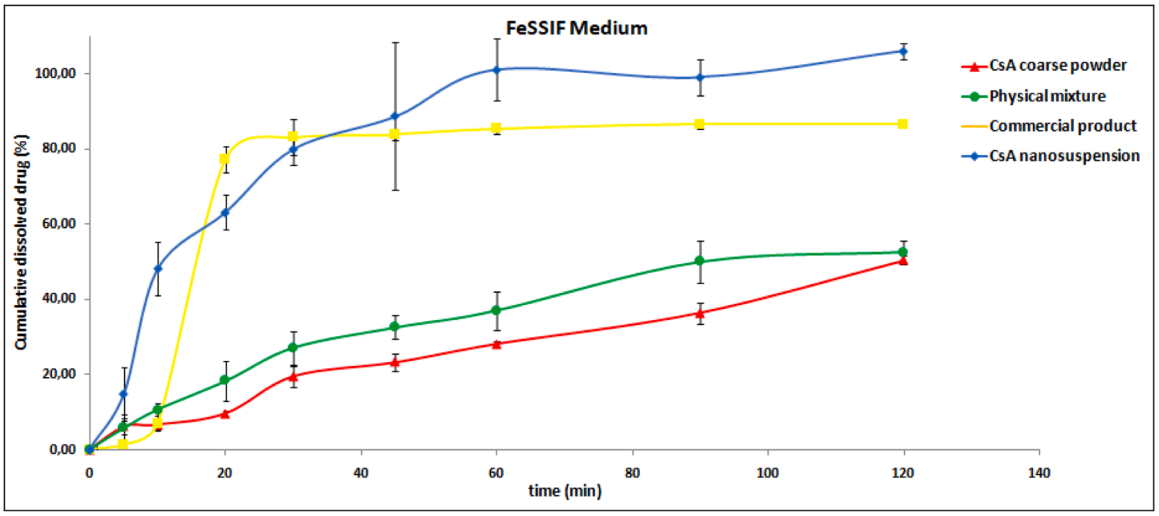

Fig. 10. Dissolution profiles of CsA coarse powder, physical mixture, CsA nanosuspension, and the commercial product in FeSSIF medium.

100% dissolution after 120 min. Additionally, CsA nanosuspension showed 35% dissolution and CsA nanosuspension improved dissolution of CsA coarse powder in this medium. Dissolution profiles obtained from the two media proved that the dissolution differences observed between 0.1 N HCl medium and 0.1 N HCl medium containing 0.5% SDS are caused by the existence of SDS (Fig. 8A and B). In another study performed in our laboratory, it has been shown that SLS is a surfactant that increases dissolution in nanosuspension formulations in dissolution studies performed in media with different ratios of SLS (Tashan et al., 2019).

Nanosuspensions can reduce variation of drugs with low water solubility such as BCS Class II in fasted/fed as well as increase their water solubility with nanosized particle size (Tashan et al., 2019; Karaküçük et al., 2019; Rodriguez Amado et al., 2017; Roos et al., 2018). In vitro dissolution studies were also performed in FaSSIF and FeSSIF media (biorelevant media) to evaluate the in vivo performance of CsA in fasted and fed conditions due to the variation in the bioavailability of CsA in the fasted/fed state. Biorelevant media is frequently used in the evaluation of many BCS class II drugs (Fagerberg et al., 2010; Yılmaz Usta et al., 2018). In vitro dissolution studies were performed in FaSSIF and FeSSIF media (biorelevant media) to evaluate the simulation of in vivo performance of CsA in fasted and fed conditions. In dissolution studies performed in biologically relevant media such as FaSSIF and FeSSIF, samples are filtered or centrifuged. In this study, it was preferred to filter the samples according to the literature (Sarısaltık Yaşın et al., 2018; Tashan et al., 2019; Karakucuk et al., 2016). Dissolution profiles obtained from the two biorelevant media were illustrated in Figs. 9 and 10. As shown in Fig. 9, in the dissolution studies carried out in FaSSIF medium, CsA coarse powder and physical mixture showed 15% and 20% dissolution, at the end of the sampling point, respectively. The physical mixture showed more dissolution than coarse powder due to the solubility increasing properties of surfactant stabilizer SDS. Both CsA nanosuspension and the commercial product showed 80% dissolution in FaSSIF medium in 120 min.

In the other biorelevant media, FeSSIF medium, CsA coarse powder, and physical mixture showed approximately 40% dissolution at the last sampling point similarly. While the commercial product showed 80% dissolution; the highest dissolution was found with about 100% with CsA nanosuspension in 120 min in FeSSIF medium (Fig. 10).

As a result of dissolution studies performed in biorelevant media, CsA nanosuspension showed higher dissolution in both media compared to CsA coarse powder. Also, CsA nanosuspensions could be used to

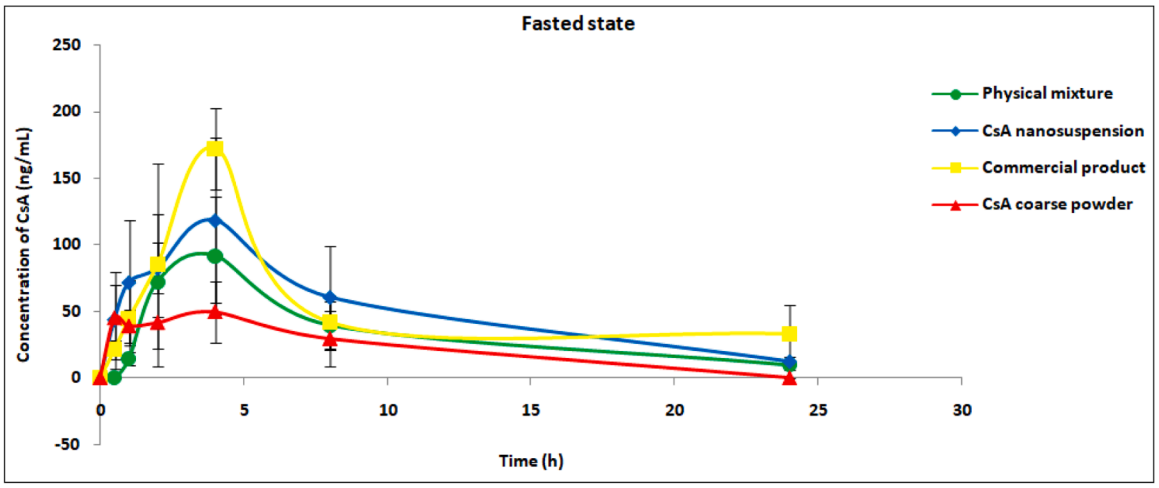

Fig. 11. The mean plasma concentration vs. time profiles of samples after oral administration in the fasted group (mean±SD, $n = 4$).

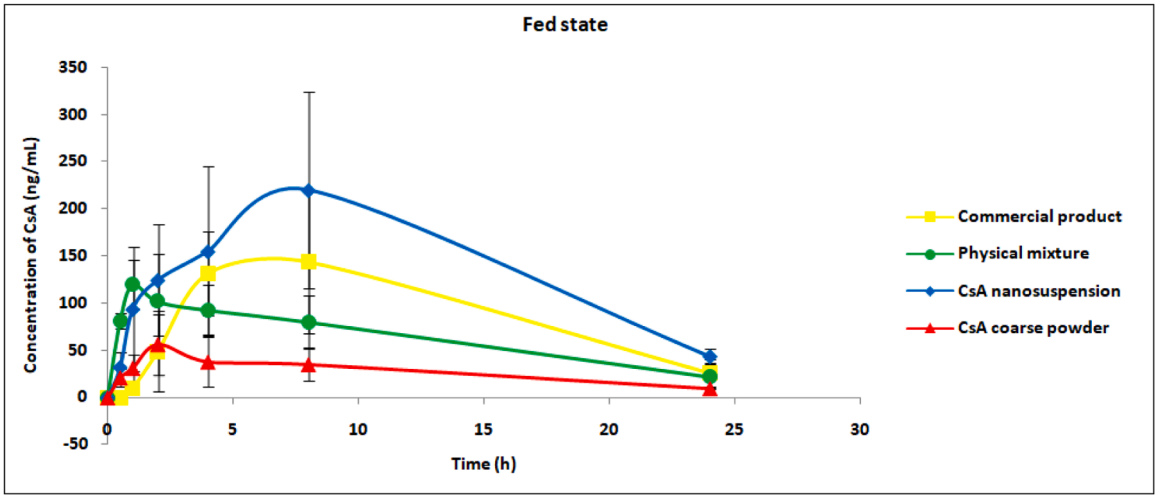

Fig. 12. The mean plasma concentration vs. time profiles of samples after oral administration in the fed group (mean±SD, $n = 4$).

decrease fasted/fed state variation by increasing dissolution than the commercial product in FeSSIF media. In accordance with the Noyes-Whitney equation, as a result of the decreasing of the particle size, an increase in the particle surface area occurs and this increase results in an increase in the dissolution rate.

3.8. Pharmacokinetic assessments

Nanosuspensions are a promising candidate for improving the bioavailability of drugs which has low bioavailability and for decreasing the variation of fasted and fed state after oral administration (Rahim et al., 2019). In a study by Persson et al., the effect of food on the absorption and bioavailability of low-soluble drugs, including cyclosporine, was investigated with intestinal pig perfusion model. In the study; the effect of food-drug interaction on solubility was found to be more significant than inhibition of P-glycoprotein (P-gp) (Persson et al., 2008).

In the fasted bioavailability study, CsA coarse powder, physical mixture, CsA nanosuspension, and the commercial product were administered to the overnight fasted rats by oral gavage dispersed with distilled water at a dose of 10 mg/kg body weight of the animal. The blood samples were taken from the tail veins at the determined time points and were analyzed for drug content by the validated LC-MS/MS method.

Table 5
Pharmacokinetic parameters of CsA in fasted and fed groups (mean±SD, $n = 4$).

Group	Samples	$t_{1/2}$(h)	t_{max}(h)	C_{max}(ng/mL)	AUC_{0-24}(h.ng/mL)	MRT(h)
Fasted	*CsA coarse powder*	5.033 ± 0.406	2.250 ± 2.021	64.522 ± 7.516	542.095 ± 346.182	6.795 ± 3.985
	Physical mixture	9.329 ± 4.167	2.375 ± 1.887	107.627 ± 27.341	862.521 ± 282.232	8.328 ± 1.290
	CsA nanosuspension	8.906 ± 3.114	2.750 ± 1.500	136.715 ± 31.265	1133.231 ± 505.129	8.250 ± 0.430
	Commercial product	18.580 ± -	3.500 ± 1.000	174.010 ± 31.913	1266.773 ± 436.188	9.233 ± 0.803
Fed	*CsA coarse powder*	15.968 ± -	2.250 ± 1.258	59.804 ± 29.333	525.380 ± 184.131	8.628 ± 3.364
	Physical mixture	8.144 ± 2.319	2.000 ± 1.414	138.280 ± 23.426	1424.370 ± 454.624	8.912 ± 1.145
	CsA nanosuspension	13.763 ± -	6.250 ± 3.500	238.434 ± 78.692	2895.135 ± 924.102	10.310 ± 0.839
	Commercial product	–	4.500 ± 2.517	168.486 ± 51.002	1672.460 ± 830.509	8.755 ± 2.962

The mean plasma levels of CsA in the fasted group after oral administration of a single dose of coarse powder, physical mixture, CsA nanosuspension, and the commercial product were shown in Fig. 11.

The mean plasma levels of CsA in the fed group after oral administration of a single dose of coarse powder, physical mixture, commercial product, and CsA nanosuspension were shown in Fig. 12.

According to the Figs. 11 and 12, the inter-subject variations and standard deviations were found to be high since CsA has both high fasted-fed variation and high inter-individual variation. To estimate the food effect, the pharmacokinetic parameters including $t_{1/2}$, t_{max}, C_{max}, $AUC_{0–24}$, and MRT in fasted and fed groups are shown in Table 5.

In fasted condition, CsA nanosuspension showed 136.715±31.265 ng/mL and 1133.231±505.129 h.ng/mL for C_{max} and $AUC_{0–24}$, respectively. CsA nanosuspension increased C_{max} for 2.12 and 1.27-fold and $AUC_{0–24}$ for 2.09 and 1.31-fold compared to the CsA coarse powder and physical mixture, respectively. The commercial product showed slightly higher C_{max} and $AUC_{0–24}$ with 174.010±31.13 ng/mL and 1266.773±436.188 h.ng/mL, respectively. These results were similar to in vitro dissolution results obtained with FaSSIF media (Fig. 9).

In fed condition, CsA nanosuspension showed 238.434±78.692 ng/mL and 2895.135±924.102 h.ng/mL for C_{max} and $AUC_{0–24}$, respectively. C_{max} value was higher 3.99, 1.72, and 1.42-fold as well as $AUC_{0–24}$ value was higher 5.51, 2.03, and 1.73-fold compared to the CsA coarse powder, physical mixture, and commercial product, respectively (Table 5). These results were also similar to in vitro dissolution results obtained with FeSSIF media (Fig. 10).

According to the Table 5, high standard deviation values in both fasted and fed condition shows that CsA is a highly variable drug that varies widely within and between individuals. The pharmacokinetic parameters indicated that food intake affected the bioavailability of CsA in samples. Increased C_{max} and $AUC_{0–24}$ values obtained with CsA nanosuspension in both fasted and fed state; proves that nanosuspensions increase the solubility, dissolution, and bioavailability of active ingredients. In a study conducted by Li et al. in 2020, magnolol nanosuspensions were prepared using Soluplus and Poloxamer 188. Magnolol nanosuspensions increased C_{max} 2.13-fold and $AUC_{0-\infty}$ 2.34-fold compared to free magnolol (Li et al., 2020).

According to the Table 5, the increase in the pharmacokinetic parameters of the physical mixture is thought to be due to the effect of the excipients used, similar to in the in vitro dissolution studies. Although CsA nanosuspension showed slightly lower $AUC_{0–24}$ compared to the commercial product in the fasted condition, it showed approximately 2-fold higher $AUC_{0–24}$ in the fed condition. Similarly, in a study conducted with ritonavir (RTV), higher bioavailability was found in RTV nanosuspensions in the fed state compared to the fasting state, and it was thought that the solubility of RTV may be increased due to the higher pH in the fed state (Karaküçük et al., 2019).

In a study performed with CsA, nanosuspensions were prepared with pearl milling technique using zirconium oxide beads as a milling media for intravenous (iv) administration of CsA, and Poloxamer 407 was used as a stabilizer. After in vivo studies were carried out in albino rats after iv administration and the pharmacokinetic parameters were indicated that the prepared formulation had better results than the marketed one (Nakarani et al., 2010).

3.9. Immunological evaluation

There are many studies conducted in rats and mice to investigate the immunomodulatory effect of CsA (Marino et al., 2011; Diaz-Romero et al., 2001). In this study, the effect of the prepared CsA nanosuspension on the immune system was compared with the commercial product. Results of immunological studies are given below.

3.9.1. Lymphocyte subsets and analysis of flow cytometry

Flow cytometry results were shown in Fig. 13. In experimental groups where CsA nanosuspension was administered for 7, 14, and 21

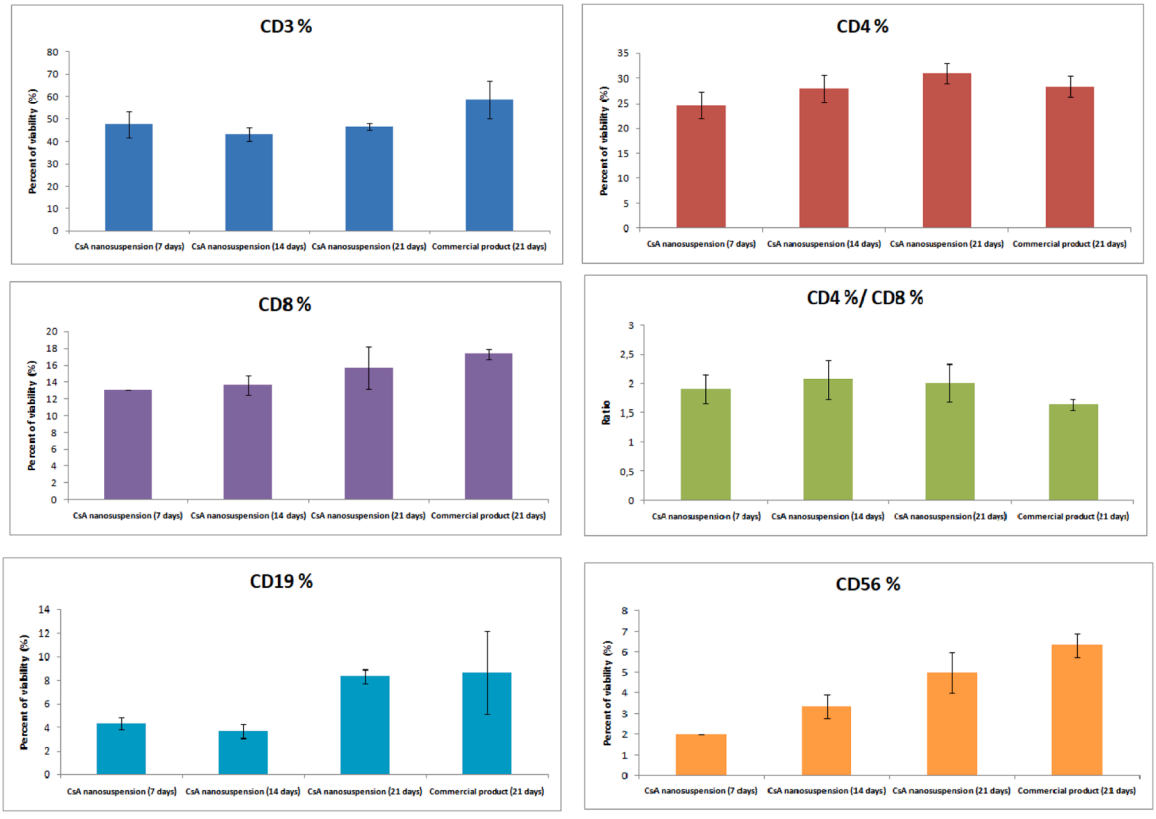

Fig. 13. Percent of viability for T lymphocyte subsets (CD3, CD4, CD8, CD19, and CD56) and CD4/CD8 ratio after oral CsA nanosuspension and the commercial product administration.

days, the alter in CD3+ T cells, CD4+ helper T cells, and CD8+ cytotoxic T cells were found statistically insignificant ($p>0.05$). CD4/CD8 ratio was 1.90 for CsA nanosuspension administered for 7 days, CD4/CD8 ratio was 2.06 for CsA nanosuspension administered for 14 days, while this ratio was 2.01 for CsA nanosuspension administered for 21 days, this difference between days was statistically insignificant ($p>0.05$). At the end of the 21 days, the difference in the ratio of CD4+/CD8+ between the commercial product and CsA nanosuspension groups was found to be statistically insignificant ($p> 0.005$).

In the groups where CsA nanosuspensions were administered, there was a significant increase in CD19+ B cells with 21 days of administration ($p<0.001$). It was found that there was no significant difference ($p> 0.05$) in the CD19+ cell percentage in the commercial product group with the group in which CsA nanosuspension was administered for 21 days. It was found that the rate of CD56+ NK cells increased from 2% to 5% over time in groups in which CsA nanosuspensions were administered during the experiment period and this increase was significant. CD56+ cell ratio was 6.3% in the group in which the commercial products were administered for 21 days. In vivo immunological study results showed that CsA formulations administered orally at a dose equivalent to 10 mg/kg once a day did not affect the distribution of T cell subgroups and B cells. As a result of the administration under the same conditions, it was found that the CD4+/CD8+ ratio increased in 7 and 14 days. Our study results show that the CsA nanosuspension dose we used in our study has no immunosuppressive effect on CD4+ helper T cells. The main target of CsA is the T helper subsets (Flores et al., 2019). Therefore to explain the increase of the CD4+/CD8+ ratio more studies are needed to increase our knowledge of the immunological effects of

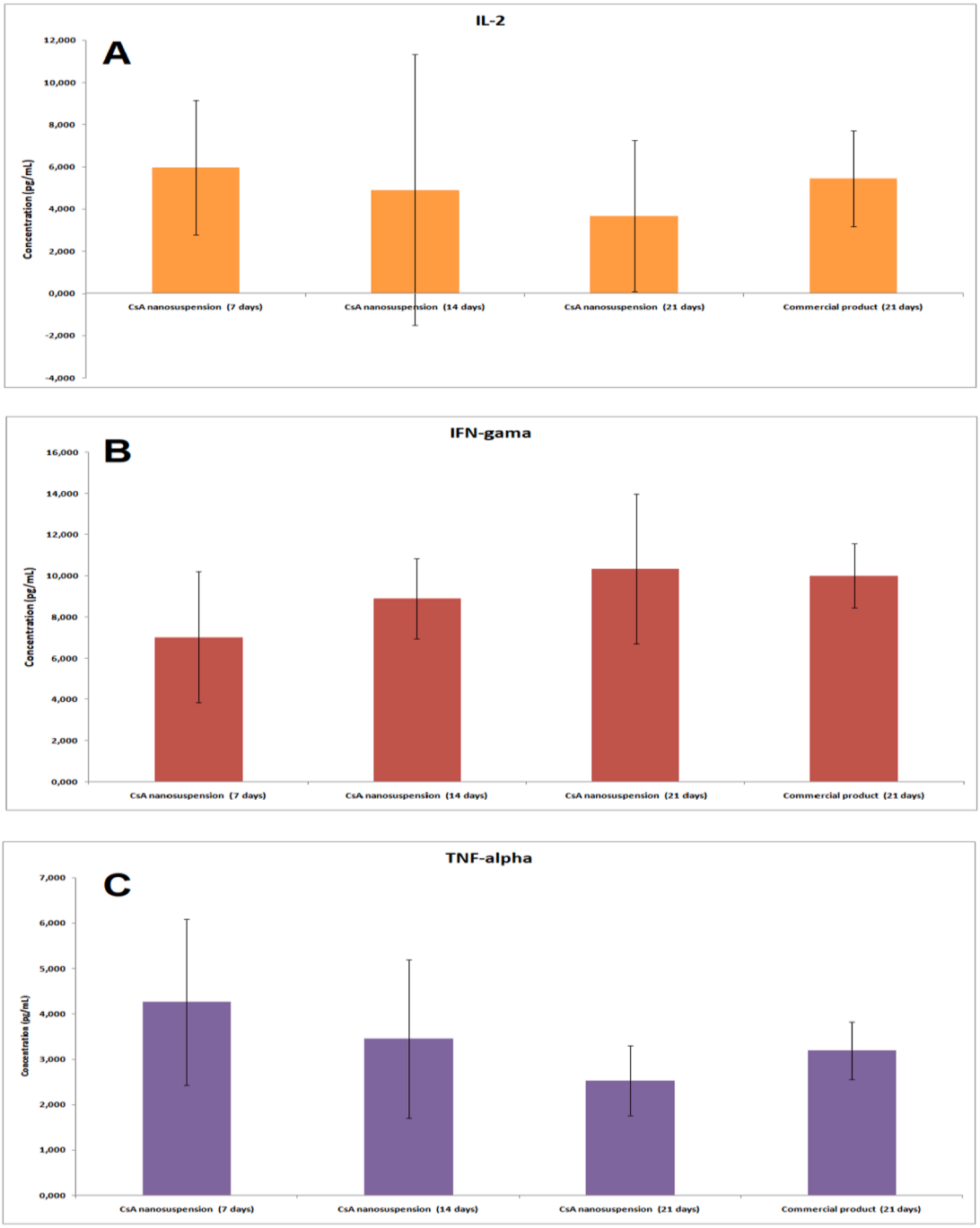

Fig. 14. IL-2, IFN-gamma, and TNF-alpha values of rat groups treated with CsA nanosuspension and the commercial product.

CsA on T cell subgroups, such as Th1, CD4+ CD25+ T reg cells.

3.9.2. Immune cell subsets and analysis of multiplex immunoassay

IL-2, IFN-gamma, and TNF-alpha results were shown in Fig. 14. As seen in Fig. 14A; from day 7 to day 21, there was a decrease in IL-2 level in the group treated with nanosuspension; at the end of the 21st day, the level of IL-2 in the group treated with nanosuspension was lower than the group treated with the commercial product. Similar to IL-2 results; from the 7th day to the 21st day, a decrease occurred in the TNF-alpha level in the group treated with nanosuspension, and at the end of the 21st day the TNF-alpha level in the group treated with nanosuspension was lower than the group treated with the commercial product (Fig. 14C). As shown in Fig. 14B; there was an increase in IFN-gamma level from day 7 to day 21 in the nanosuspension group. At the end of the 21st day of administration, the IFN-gamma level was found to be slightly higher in rats treated with the nanosuspension compared to rats treated with the commercial products.

According to Figs. 13 and 14; there appears to be a decrease in T cells, CD8 cells, CD56 cells, and NK cells, owing to the lower IL-2 level seen in rats treated with CsA nanosuspension compared to rats treated with the commercial product (Acker et al., 2017). The lower IL-2 level seen in rats treated with CsA nanosuspension may indicate that the immunosuppressive effect is maintained a longer and higher immunosuppression is seen, however, this study should be supported by further studies.

4. Conclusion

CsA nanosuspensions were successfully prepared by the wet media milling method which of top-down production technology. The increased water solubility and dissolution in FaSSIF and FeSSIF media of CsA according to coarse powder and physical mixture were obtained with nanosuspension. CsA nanosuspension dissolved almost completely and showed higher dissolution than the commercial product in FeSSIF medium at the end of the sampling points.

Pharmacokinetic and immunological studies of the successfully prepared CsA nanosuspension according to the characterization, solubility and dissolution results were evaluated. The pharmacokinetic study in rats indicated that C_{max} values of CsA nanosuspension were to be 2.12 and 3.99-fold higher than CsA coarse powder in fasted and fed conditions, respectively. These results suggesting that a significant increase in CsA bioavailability was obtained with nanosuspension. Immunological studies in rats proved that CsA nanosuspension was found to be more acceptable by the means of the CD4+/CD8+ ratio than the commercial product. In conclusion, this study demonstrated that the nanosuspension produced by wet milling could be a promising strategy to improve solubility and dissolution of CsA for oral administration and to reduce intra and inter individual variation.

CRediT authorship contribution statement

Sıla Gülbağ Pınar: Conceptualization, Methodology, Validation, Formal analysis, Investigation, Writing – review & editing, Visualization. **Hande Canpınar:** Methodology, Validation, Writing – original draft. **Çağman Tan:** Methodology, Validation, Writing – original draft. **Nevin Çelebi:** Conceptualization, Methodology, Validation, Formal analysis, Investigation, Writing – review & editing, Supervision, Project administration.

Declaration of competing interest

No potential conflict of interest was reported by the authors.

Acknowledgment

This study was supported by Gazi University Scientific Research Project Foundation (Grant No:02/2017–14). The authors are thankful to Deva Drug Company (İstanbul, Turkey) for providing CsA. The authors also thank Assoc. Prof. Mürşide Ayşe Demirel for contributing the in vivo study.

References

Acker, H.H.V., Capsomidis, A., Smits, E.L., Tendeloo, V.F.V., 2017. CD56 in the Immune system: more than a marker for cytotoxicity? Front. Immunol 8, 892. https://doi.org/10.3389/fimmu.2017.00892.

Ahire, E., Thakkar, S., Darshanwad, M., Misra, M., 2018. Parenteral nanosuspensions: a brief review from solubility enhancement to more novel and specific applications. Acta Pharmaceutica Sinica B 8, 733–755. https://doi.org/10.1016/j.apsb.2018.07.011.

Aljohani, B., Alotaibi, F.F., Ghazaly, E., Jaber, J.A., Perrett, D., Johnston, A., 2017. Development and validation of A HPLC-UV method for dissolution testing of ciclosporin: its application to the measurement of brand and generic versions from different countries. J. Bioequiv. Availab. 09 https://doi.org/10.4172/jbb.1000354.

Amidon, G.L., Lennernas, H., Shah, V.P., Crison, J.R., 1995. A theoretical basis for a biopharmaceutic drug classification: the correlation of in vitro drug product dissolution and in vivo bioavailability. Pharm. Res. 12, 413–420. https://doi.org/10.1023/a:1016212804288.

Ao, H., Li, Y., Li, H., Wang, Y., Han, M., Guo, Y., Shi, R., Yue, F., Wang, X., 2020. Preparation of hydroxy genkwanin nanosuspensions and their enhanced antitumor efficacy against breast cancer. Drug Deliv. 27 (1), 816–824. https://doi.org/10.1080/10717544.2020.1770372.

Attari, Z., Bhandari, A., Jagadish, P.C., Lewis, S., 2016. Enhanced ex vivo intestinal absorption of olmesartan medoxomil nanosuspension: preparation by combinative technology. Saudi Pharmac. J. 24, 57–63. https://doi.org/10.1016/j.jsps.2015.03.008.

Balandraud-Pieri, N., Queneau, P.E., Caroli-Bosc, F.X., Bertault-Peres, P., Montet, A.M., Durand, A., Montet, J.C., 1997. Effects of tauroursodeoxycholate solutions on cyclosporin A bioavailability in rats. Drug Metab. Dispos 25, 912–916.

Basaran, E., Yenilmez, E., Berkman, M.S., Buyukkoroglu, G., Yazan, Y., 2014. Chitosan nanoparticles for ocular delivery of cyclosporine A. J. Microencapsul. 31, 49–57. https://doi.org/10.3109/02652048.2013.805839.

Cheng, Y., Lin, B.J., Guo, J.H., Huang, B.L., Fang, L.P., Que, W.C., Liu, M.B., Chen, X.F., Qiu, H.Q., 2019. The effect of food on the pharmacokinetic properties and bioequivalence of two formulations of levocetirizine dihydrochloride in healthy chinese volunteers. Drug Des. Devel. Ther. 13, 3625–3634. https://doi.org/10.2147/DDDT.S215316.

Christians, U., Sewing, K.F., 1993. Cyclosporin metabolism in transplant patients. Pharmacol. Ther. 57, 291–345. https://doi.org/10.1016/0163-7258(93)90059-M.

da Silva Peralta, F., Pallos, D., Silva Queiroz, C., Ricardo, L.H., 2015. Previous exposure to Cyclosporine A and periodontal breakdown in rats. Arch. Oral Biol. 60, 566–573. https://doi.org/10.1016/j.archoralbio.2015.01.004.

Diaz-Romero, J., Vogt, G., Weckbecker, G., 2001. Coexpression of CD4 and CD8α on rat T-cells in whole blood: a sensitive marker for monitoring T-cell immunosuppressive drugs. J. Immunol. Methods 254, 1–12. https://doi.org/10.1016/s0022-1759(01)00363-5. V.

Ding, Z., Wang, L., Xing, Y., Zhao, Y., Wang, Z., Han, J., 2019. Enhanced oral bioavailability of celecoxib nanocrystalline solid dispersion based on wet media milling technique: formulation, optimization and In Vitro/In Vivo evaluation. Pharmaceutics 11. https://doi.org/10.3390/pharmaceutics11070328.

Fagerberg, J.H., Tsinman, O., Sun, N., Tsinman, K., Avdeef, A., Bergstrom, C.A., 2010. Dissolution rate and apparent solubility of poorly soluble drugs in biorelevant dissolution media. Mol Pharm 7, 1419–1430. https://doi.org/10.1021/mp100049m.

Fahr, A., 1993. Cyclosporin clinical pharmacokinetics. Clin Pharmacokinet 24, 472–495. https://doi.org/10.2165/00003088-199324060-00004.

Flippin, M.S., Canter, C.E., Balzer, D.T., 2000. Increased morbidity and high variability of cyclosporine levels in pediatric heart transplant recipients. J. Heart Lung Transp. 19, 343–349. https://doi.org/10.1016/s1053-2498(00)00061-9.

Flores, C., Fouquet, G., Moura, I.C., Maciel, T.T., Hermine, O., 2019. Lessons to learn from low-dose cyclosporin-a: a new approach for unexpected clinical applications. Front Immunol 10, 588. https://doi.org/10.3389/fimmu.2019.00588.

Freeman, D.J., 1991. Pharmacology and pharmacokinetics of cyclosporine. Clin. Biochem. 24, 9–14. https://doi.org/10.1016/0009-9120(91)90084-R.

Fu, Q., Sun, J., Zhang, D., Li, M., Wang, Y., Ling, G., Liu, X., Sun, Y., Sui, X., Luo, C., Sun, L., Han, X., Lian, H., Zhu, M., Wang, S., He, Z., 2013. Nimodipine nanocrystals for oral bioavailability improvement: preparation, characterization and pharmacokinetic studies. Colloid. Surf. B: Biointerfaces 109, 161–166. https://doi.org/10.1016/j.colsurfb.2013.01.066.

Ghosh, I., Schenck, D., Bose, S., Ruegger, C., 2012. Optimization of formulation and process parameters for the production of nanosuspension by wet media milling technique: effect of Vitamin E TPGS and nanocrystal particle size on oral absorption. Eur. J. Pharmac. Sci. 47, 718–728. https://doi.org/10.1016/j.ejps.2012.08.011.

Guada, M., Beloqui, A., Kumar, M.N., Preat, V., Dios-Vieitez Mdel, C., Blanco-Prieto, M. J., 2016. Reformulating cyclosporine A (CsA): more than just a life cycle management strategy. J. Controll. Release 225, 269–282. https://doi.org/10.1016/j.jconrel.2016.01.056.

Gulsun, T., Borna, S.E., Vural, I., Sahin, S., 2018. Preparation and characterization of furosemide nanosuspensions. J. Drug Deliv. Sci. Technol. 45, 93–100. https://doi.org/10.1016/j.jddst.2018.03.005.

Gülbağ Pınar, S., Çelebi, N., 2019. Optimization and evaluation of cyclosporine A nanosuspension stabilized by combination stabilizers using high pressure homogenization method. J. Res. Pharmacy 23, 1009–1021. https://doi.org/10.35333/jrp.2019.65.

Handschumacher, R.E., Harding, M.W., Rice, J., Drugge, R.J., Speicher, D.W., 1984. Cyclophilin: a specific cytosolic binding protein for cyclosporin A. Science 226 (4674), 544–547. https://doi.org/10.1126/science.6238408. Nov 2.

He, J., Han, Y., Xu, G., Yin, L., Ngandeu Neubi, M., Zhou, J., Ding, Y., 2017. Preparation and evaluation of celecoxib nanosuspensions for bioavailability enhancement. RSC Adv 7, 13053–13064. https://doi.org/10.1039/C6RA28676C.

Hermans, K., Van den Plas, D., Everaert, A., Weyenberg, W., Ludwig, A., 2012. Full factorial design, physicochemical characterisation and biological assessment of cyclosporine A loaded cationic nanoparticles. Eur. J. Pharm. Biopharm. 82, 27–35. https://doi.org/10.1016/j.ejpb.2012.05.003.

Hong, C., Dang, Y., Lin, G., Yao, Y., Li, G., Ji, G., Shen, H., Xie, Y., 2014. Effects of stabilizing agents on the development of myricetin nanosuspension and its characterization: an in vitro and in vivo evaluation. Int. J. Pharm. 477, 251–260. https://doi.org/10.1016/j.ijpharm.2014.10.044.

Huang, S., Zhang, Q., Li, H., Sun, Y., Cheng, G., Zou, M., Piao, H., 2018. Increased bioavailability of efonidipine hydrochloride nanosuspensions by the wet-milling method. Eur. J. Pharm. Biopharm. 130, 108–114. https://doi.org/10.1016/j.ejpb.2018.06.022.

Italia, J.L., Bhatt, D.K., Bhardwaj, V., Tikoo, K., Kumar, M.N., 2007. PLGA nanoparticles for oral delivery of cyclosporine: nephrotoxicity and pharmacokinetic studies in comparison to Sandimmune Neoral. J. Control. Release 119, 197–206. https://doi.org/10.1016/j.jconrel.2007.02.004.

Iyama, Y., Mineda, M., Sei, S., Hirasawa, W., Matahira, Y., Seto, Y., Sato, H., Onoue, S., 2019. Cyclosporine a-loaded UniORV(R): pharmacokinetic and safety characterization. Int. J. Pharm. 570, 118630 https://doi.org/10.1016/j.ijpharm.2019.118630.

Jain, S., Mittal, A., Jain, A.K., 2011. Enhanced topical delivery of Cyclosporin-A Using PLGA nanoparticles as carrier. Curr. Nanosci. 7, 524–530. https://doi.org/10.2174/157341311796196835.

Junghanns, J.U., Müller, R.H., 2008. Nanocrystal technology, drug delivery and clinical applications. Int. J. Nanomed.e 3, 295–309. https://doi.org/10.2147/ijn.s595.

Junyaprasert, V.B., Morakul, B., 2015. Nanocrystals for enhancement of oral bioavailability of poorly water-soluble drugs. Asian J. Pharmac. Sci. 10, 13–23. https://doi.org/10.1016/j.ajps.2014.08.005.

Karakucuk, A., Celebi, N., 2020. Investigation of Formulation and Process Parameters of Wet Media Milling to Develop Etodolac Nanosuspensions. Pharm. Research 37, 111. https://doi.org/10.1007/s11095-020-02815-x.

Karakucuk, A., Celebi, N., Teksin, Z.S., 2016. Preparation of ritonavir nanosuspensions by microfluidization using polymeric stabilizers: I. A design of experiment approach. Eur. J. Pharmac. Sci. 95, 111–121. https://doi.org/10.1016/j.ejps.2016.05.010.

Karakucuk, A., Ozturk, N., Celebi, N., 2020. Evaluation of Caco-2 cell permeability of ritonavir nanosuspensions. Istanbul J. Pharm. 50 (3), 251–255. https://doi.org/10.26650/IstanbulJPharm.2020.0028.

Karakucuk, A., Teksin, Z.S., Eroglu, H., Celebi, N., 2019. Evaluation of improved oral bioavailability of ritonavir nanosuspension. Eur. J. Pharm. Sci. 131, 153–158. https://doi.org/10.1016/j.ejps.2019.02.028.

Karakucuk, A., Tort, S., Han, S., Oktay, A.N., Celebi, N., 2021. Etodolac nanosuspension based gel for enhanced dermal delivery: in vitro and in vivo evaluation. J. Microencapsul. 38 (4), 218–232. https://doi.org/10.1080/02652048.2021.1895344.

Kobayashi, M., Kondo, K., Nakashima, C., Kida, Y., Niwa, T., 2020. Design of self-dispersible microsponge containing cyclosporine through wet milling and drop freeze-drying processes to improve dissolution behavior. J. Drug Deliv. Sci. Tec. 57, 1773–2247. https://doi.org/10.1016/j.jddst.2020.101577.

Koradia, K.D., Sheth, N.R., Koradia, H.D., Dabhi, M.R., 2018. Ziprasidone nanocrystals by wet media milling followed by spray drying and lyophilization: formulation and process parameter optimization. J. Drug Deliv. Sci. Tec. 43, 73–84. https://doi.org/10.1016/j.jddst.2017.09.011.

Lahiani-Skiba, M., Hallouard, F., Bounoure, F., Milon, N., Karrout, Y., Skiba, M., 2018. Enhanced Dissolution and Oral Bioavailability of Cyclosporine A: microspheres Based on alphabeta-Cyclodextrins Polymers. Pharmaceutics 10. https://doi.org/10.3390/pharmaceutics10040285.

Li, G., Lu, Y., Fan, Y., Ning, Q., Li, W., 2020. Enhanced oral bioavailability of magnolol via mixed micelles and nanosuspensions based on Soluplus®-Poloxamer 188. Drug Deliv 27 (1), 1010–1017. https://doi.org/10.1080/10717544.2020.1785582.

Li, Y., Wang, D., Lu, S., Zeng, L., Wang, Y., Song, W., Liu, J., 2018. Pramipexole nanocrystals for transdermal permeation: characterization and its enhancement micro-mechanism. Eur. J. Pharm. Sci. 124, 80–88. https://doi.org/10.1016/j.ejps.2018.08.003.

Lindholm, A., 1991. Factors influencing the pharmacokinetics of cyclosporine in man. Ther Drug Monit 13, 465–477. https://doi.org/10.1097/00007691-199111000-00001.

Liu, Q., Mai, Y., Gu, X., Zhao, Y., Di, X., Ma, X., Yang, J., 2020. A wet-milling method for the preparation of cilnidipine nanosuspension with enhanced dissolution and oral bioavailability. J. Drug Deliv. Sci. Tec. 55, 101371 https://doi.org/10.1016/j.jddst.2019.101371.

Marino, A., Plaza, D., Delgado, D., 2011. Preliminary study to characterize differences in potential immunomodulatory effects of cyclosporine A using BALB/c and ICR mouse splenocytes. Brazil. J. Pharmac. Sci. 47 (1), 175–183. https://doi.org/10.1590/S1984-82502011000100022.

Mauludin, R., Müller, R.H., Keck, C.M., 2009. Development of an oral rutin nanocrystal formulation. Int. J. Pharm. 370, 202–209. https://doi.org/10.1016/j.ijpharm.2008.11.029.

Medarevic, D., Djuris, J., Ibric, S., Mitric, M., Kachrimanis, K., 2018. Optimization of formulation and process parameters for the production of carvedilol nanosuspension by wet media milling. Int. J. Pharm. 540, 150–161. https://doi.org/10.1016/j.ijpharm.2018.02.011.

Möschwitzer, J.P., 2013. Drug nanocrystals in the commercial pharmaceutical development process. Int. J. Pharm. 453, 142–156. https://doi.org/10.1016/j.ijpharm.2012.09.034.

Müller, R.H., Gohla, S., Keck, C.M., 2011. State of the art of nanocrystals - special features, production, nanotoxicology aspects and intracellular delivery. Eur. J. Pharm. Biopharm. 78, 1–9. https://doi.org/10.1016/j.ejpb.2011.01.007.

Nakarani, M., Patel, P., Patel, J., Patel, P., Murthy, R.S.R., Vaghani, S.S., 2010. Cyclosporine A-nanosuspension: formulation, characterization and In Vivo comparison with a marketed formulation. Sci. Pharm. 78 (2), 345–361. https://doi.org/10.3797/scipharm.0908-12.

National Center for Biotechnology Information, 2021. PubChem compound summary for ID 5280754. Cyclosporine. Retrieved November 21, 2021 from. pubchem.ncbi.nlm.nih.gov/compound/Cyclosporine.

Oktay, A.N., Karakucuk, A., Ilbasmis-Tamer, S., Celebi, N., 2018. Dermal flurbiprofen nanosuspensions: optimization with design of experiment approach and in vitro evaluation. Eur. J. Pharm. Sci. 122, 254–263. https://doi.org/10.1016/j.ejps.2018.07.009.

Oktay, A.N., Ilbasmis-Tamer, S., Han, S., Uludag, O., Celebi, N., 2020. Preparation and in vitro /in vivo evaluation of flurbiprofen nanosuspension-based gel for dermal application. Eur. J. Pharm. Sci. 155, 105548 https://doi.org/10.1016/j.ejps.2020.105548.

Omachi, F., Kaneko, M., Iijima, R., Watanabe, M., Itagaki, F., 2019. Relationship between the effects of food on the pharmacokinetics of oral antineoplastic drugs and their physicochemical properties. J. Pharm. Health Care Sci. 5, 26. https://doi.org/10.1186/s40780-019-0155-1.

Onoue, S., Sato, H., Ogawa, K., Kawabata, Y., Mizumoto, T., Yuminoki, K., Hashimoto, N., Yamada, S., 2010. Improved dissolution and pharmacokinetic behavior of cyclosporine A using high-energy amorphous solid dispersion approach. Int. J. Pharm. 399, 94–101. https://doi.org/10.1016/j.ijpharm.2010.08.007.

Patel, D., Zode, S.S., Bansal, A.K., 2020. Formulation aspects of intravenous nanosuspensions. Int. J. Pharm. 586, 119555 https://doi.org/10.1016/j.ijpharm.2020.119555.

Persson, E.M., Nordgren, A., Forsell, P., Knutson, L., Öhgren, C., Forssén, S., Lennernäs, H., Abrahamsson, B., 2008. Improved understanding of the effect of food on drug absorption and bioavailability for lipophilic compounds using an intestinal pig perfusion model. Eur. J. Pharm. Sci. 34 (1), 22–29. https://doi.org/10.1016/j.ejps.2008.02.002.

Rahim, H., Sadiq, A., Khan, S., Amin, F., Ullah, R., Shahat, A.A., Mahmood, H.M., 2019. Fabrication and characterization of glimepiride nanosuspension by ultrasonication-assisted precipitation for improvement of oral bioavailability and in vitro alpha-glucosidase inhibition. Int. J. Nanomedicine 14, 6287–6296. https://doi.org/10.2147/IJN.S210548.

Rodriguez Amado, J.R., Prada, A.L., Duarte, J.L., Keita, H., da Silva, H.R., Ferreira, A.M., Sosa, E.H., Carvalho, J.C.T., 2017. Development, stability and in vitro delivery profile of new loratadine-loaded nanoparticles. Saudi Pharm. J. 25, 1158–1168. https://doi.org/10.1016/j.jsps.2017.07.008.

Roos, C., Dahlgren, D., Sjogren, E., Sjoblom, M., Hedeland, M., Lennernas, H., 2018. Jejunal absorption of aprepitant from nanosuspensions: role of particle size, prandial state and mucus layer. Eur. J. Pharm. Biopharm. 132, 222–230. https://doi.org/10.1016/j.ejpb.2018.09.022.

Sarısaltık Yaşın, D., Yılmaz, Ş., Teksin, Z.Ş., 2018. Evaluation of biorelevant media to investigate the dissolution properties on flurbiprofen and to assess cytotoxicity effects on Caco-2 cell line. Istanbul J. Pharm. 48 (3), 82–88. https://doi.org/10.26650/IstanbulJPharm.2018.180013.

Survase, S.A., Kagliwal, L.D., Annapure, U.S., Singhal, R.S., 2011. Cyclosporin A–a review on fermentative production, downstream processing and pharmacological applications. Biotechnol. Adv. 29, 418–435. https://doi.org/10.1016/j.biotechadv.2011.03.004.

Tashan, E., Karakucuk, A., Celebi, N., 2019. Optimization and in vitro evaluation of ziprasidone nanosuspensions produced by a top-down approach. J. Drug Deliv. Sci. Technol. 52, 37–45. https://doi.org/10.1016/j.jddst.2019.04.024.

Toziopoulou, F., Malamatari, M., Nikolakakis, I., Kachrimanis, K., 2017. Production of aprepitant nanocrystals by wet media milling and subsequent solidification. Int. J. Pharm. 533, 324–334. https://doi.org/10.1016/j.ijpharm.2017.02.065.

Xu, X., Gupta, A., Faustino, P., Sathe, P.M., Sayeed, V.A., Khan, M.A., 2013. Development and validation of a HPLC method for dissolution and stability assay of liquid-filled cyclosporine capsule drug products. AAPS PharmSciTech 14, 959–967. https://doi.org/10.1208/s12249-013-9983-8.

Yamasaki, K., Kwok, P.C., Fukushige, K., Prud'homme, R.K., Chan, H.K., 2011. Enhanced dissolution of inhalable cyclosporine nano-matrix particles with mannitol as matrix former. Int. J. Pharm. 420, 34–42. https://doi.org/10.1016/j.ijpharm.2011.08.010.

Yang, S.G., Kim, D.D., Chung, S.J., Shim, C.K., 2006. Stable bioavailability of cyclosporin A, regardless of food intake, from soft gelatin capsules containing a new self-nanoemulsifying formulation. Int. J. Clin. Pharmacol. Ther. 44, 233–239. https://doi.org/10.5414/cpp44233.

Yılmaz Usta, D., Demirtaş, Ö., Ökçelik, C., Uslu, A., Teksin, Z.Ş, 2018. Evaluation of in vitro dissolution characteristics of flurbiprofen, a BCS Class IIa Drug Fabad. J. Pharm. Sci. 43, 27–34.

Zakowiecki, D., Cal, K., Kaminski, K., Adrjanowicz, K., Swinder, L., Kaminska, E., Garbacz, G., 2015. The improvement of the dissolution rate of ziprasidone free base from solid oral formulations. AAPS PharmSciTech 16 (4), 922–933. https://doi.org/10.1208/s12249-015-0285-1.

Zong, L., Li, X., Wang, H., Cao, Y., Yin, L., Li, M., Wei, Z., Chen, D., Pu, X., Han, J., 2017. Formulation and characterization of biocompatible and stable I.V. itraconazole nanosuspensions stabilized by a new stabilizer polyethylene glycol-poly(beta-Benzyl-L-aspartate) (PEG-PBLA). Int. J. Pharm. 531, 108–117. https://doi.org/10.1016/j.ijpharm.2017.08.082.

Zuo, B., Sun, Y., Li, H., Liu, X., Zhai, Y., Sun, J., He, Z., 2013. Preparation and in vitro/in vivo evaluation of fenofibrate nanocrystals. Int. J. Pharm. 455, 267–275. https://doi.org/10.1016/j.ijpharm.2013.07.021.

Zuo, J., Barros de Araujo, G.L., Stephano, M.A., Zuo, Z., Bou-Chacra, N.A., Löbenberg, R., 2019. Design space approach in the development of esculetin nanocrystals by a small-scale wet-bead milling process. J. Drug Deliv. Sci. Technol., 101486 https://doi.org/10.1016/j.jddst.2019.101486.